Cladding Degradation Model

Spent Fuel and Waste Disposition

Prepared for
US Department of Energy
Spent Fuel and Waste Science and Technology
Patrick V. Brady and Jeralyn L. Prouty
Sandia National Laboratories
Brady D. Hanson
Pacific Northwest National Laboratory

April 29, 2022
M3SF-22SN010305125
SAND2020-xxxxx X

DISCLAIMER

This information was prepared as an account of work sponsored by an agency of the U.S. Government. Neither the U.S. Government nor any agency thereof, nor any of their employees, makes any warranty, expressed or implied, or assumes any legal liability or responsibility for the accuracy, completeness, or usefulness, of any information, apparatus, product, or process disclosed, or represents that its use would not infringe privately owned rights. References herein to any specific commercial product, process, or service by trade name, trade mark, manufacturer, or otherwise, does not necessarily constitute or imply its endorsement, recommendation, or favoring by the U.S. Government or any agency thereof. The views and opinions of authors expressed herein do not necessarily state or reflect those of the U.S. Government or any agency thereof.

Prepared by:
Sandia National Laboratories
Albuquerque, New Mexico 87185

Sandia National Laboratories is a multimission laboratory managed and operated by National Technology & Engineering Solutions of Sandia, LLC, a wholly owned subsidiary of Honeywell International Inc., for the U.S. Department of Energy's National Nuclear Security Administration under contract DE-NA0003525.

This is a technical paper that does not take into account the contractual limitations under the Standard Contract for Disposal of Spent Nuclear Fuel and/or High-Level Radioactive Waste (Standard Contract) (10 CFR Part 961). For example, under the provisions of the Standard Contract, DOE does not consider spent nuclear fuel in multi-assembly canisters to be an acceptable waste form, absent a mutually agreed to contract amendment. To the extent discussions or recommendations in this pape conflict with the provisions of the Standard Contract, the Standard Contract governs the obligations of the parties, and this paper in no manner supersedes, overrides, or amends the Standard Contract. This paper reflects technical work which could support future decision making by DOE. No inferences should be drawn from this paper regarding future actions by DOE, which are limited both by the terms of the Standard Contract and a lack of Congressional appropriations for the Department to fulfill its obligations under the Nuclear Waste Policy Act including licensing and construction of a spent nuclear fuel repository.

Revision 6
10/7/2019

APPENDIX E
NFCSC DOCUMENT COVER SHEET[1]

Name/Title of Deliverable/Milestone/Revision No. Cladding Degradation Model

Work Package Title and Number Probabilistic Post-Closure DPC Criticality Consequence Analysis SF-22SN01030512

Work Package WBS Number 1.08.01.03.05

Responsible Work Package Manager Laura Price *Laura Price*
(Name/Signature)

Date Submitted April 29, 2022

Quality Rigor Level for Deliverable/Milestone[2]	☐ QRL-1 ☐ Nuclear Data	☐ QRL-2	☐ QRL-3	☐ QRL-4 Lab QA Program[3]

This deliverable was prepared in accordance with Sandia National Laboratories
(Participant/National Laboratory Name)

QA program which meets the requirements of

☒ DOE Order 414.1 ☐ NQA-1 ☐ Other

This Deliverable was subjected to:

☒ Technical Review ☐ Peer Review

Technical Review (TR)
Review Documentation Provided

☐ Signed TR Report or,
☐ Signed TR Concurrence Sheet or,
☒ Signature of TR Reviewer(s) below

Name and Signature of Reviewers
Jessica Kruichak

Peer Review (PR)
Review Documentation Provided

☐ Signed PR Report or,
☐ Signed PR Concurrence Sheet or,
☐ Signature of PR Reviewer(s) below

Jessica Kruichak

NOTE 1: *Appendix E should be filled out and submitted with the deliverable. Or, if the PICS:NE system permits, completely enter all applicable information in the PICS:NE Deliverable Form. The requirement is to ensure that all applicable information is entered either in the PICS:NE system or by using the NFCSC Document Cover Sheet.*

- *In some cases there may be a milestone where an item is being fabricated, maintenance is being performed on a facility, or a document is being issued through a formal document control process where it specifically calls out a formal review of the document. In these cases, documentation (e.g., inspection report, maintenance request, work planning package documentation or the documented review of the issued document through the document control process) of the completion of the activity, along with the Document Cover Sheet, is sufficient to demonstrate achieving the milestone.*

NOTE 2: *If QRL 1, 2, or 3 is not assigned, then the QRL 4 box must be checked, and the work is understood to be performed using laboratory QA requirements. This includes any deliverable developed in conformance with the respective National Laboratory / Participant, DOE or NNSA-approved QA Program.*

NOTE 3: *If the lab has an NQA-1 program and the work to be conducted requires an NQA-1 program, then the QRL-1 box must be checked in the work Package and on the Appendix E cover sheet and the work must be performed in accordance with the Lab's NQA-1 program. The QRL-4 box should not be checked.*

This page is intentionally left blank.

SUMMARY

Cladding integrity must be reliably estimated, or bounded, in performance assessment efforts because radionuclide release from breached waste packages may be directly proportional to the fraction of cladding that is failed. While domestic and international repository programs currently make bounding assumptions of cladding barrier performance, there is interest in developing a cladding degradation model that takes credit in some manner for cladding barrier performance. The 2019 Research and Development (R&D) Roadmap Update (Sevougian et al. 2019) identified cladding degradation as an important gap in the Department of Energy's (DOE's) ongoing analyses of generic nuclear waste disposal concepts.

This report begins with an evaluation of cladding degradation mechanisms deemed important to assessing barrier capability. Unlike similar efforts done in the past, this evaluation accounts for the hypothetical conditions associated with direct dual-purpose canister (DPC) disposal, including conditions resulting from a postulated, in-package, steady-state criticality event. A total of 16 cladding degradation mechanisms are examined assuming direct disposal of DPCs in two different hypothetical repositories: a saturated repository in shale and an unsaturated repository in alluvium.

The evaluation results indicate that most of the cladding degradation mechanisms (e.g., stress corrosion cracking (SCC), delayed hydride cracking (DHC), creep failure, pitting and crevice corrosion, rod pressurization, and clad unzipping) have little impact on cladding persistence. However, three mechanisms—early cladding failure, general corrosion, and fluoride-enhanced corrosion—are identified for consideration as candidates to be included in a cladding degradation model.

A small amount of cladding (<0.1%) is expected to fail before disposal. The estimate includes cladding failures that occur during reactor operations, pool storage, dry storage, handling/consolidation, and transportation.

Although general corrosion is generally not significant at low temperatures, the mechanism is sensitive to high temperatures. The high temperatures (peak about 250°C) expected from a postulated in-package, steady-state criticality event in a saturated shale repository can result in rapid Zircaloy degradation rates on the order of 0.34 μm/yr. A few hundred years after onset of a postulated criticality event in a saturated shale repository, general corrosion of fuel assembly grid spacer walls and guide tubes will likely result in settling of fuel rods upon each other. This rod consolidation could exclude the water moderator and might terminate a postulated criticality event (Alsaed 2020), though it will depend upon the final configuration of the rods. Note that the predicted temperatures under nominal conditions for either geologic case or for the unsaturated alluvium repository with a steady-state criticality event are too low for general corrosion to be significant.

Below about 100°C, general corrosion can fail cladding only if the cladding is exposed to waters containing elevated dissolved fluoride levels (>5 ppm) at a low pH (<3.2). These chemical conditions for fluoride-enhanced corrosion are not expected to occur in a saturated shale repository. In contrast, the chemical conditions, though unlikely, could conceivably occur in an unsaturated alluvium repository subject to evaporative concentration due to cyclic wetting and drying. Assuming the chemical conditions are met, there must also be a plausible physical scenario for sufficient water contact with cladding inside a breached waste package. If fluoride-enhanced corrosion does occur in an unsaturated alluvium, the degradation rates would be accelerated under the slightly higher (<100°C) temperatures associated with a postulated criticality event compared to the rates under nominal conditions.

A description of a conceptual model for cladding degradation is presented along with the following recommendations for cladding degradation modeling procedures: (1) account for early failure of cladding, (2) calculate cladding degradation rates due to general corrosion, (3) predict in-package fluoride levels and pH, and (4) if warranted by fluoride levels and pH, calculate degradation rates due to fluoride-enhanced corrosion.

This page is intentionally left blank.

ACKNOWLEDGEMENTS

This work was supported by the DOE Office of Nuclear Energy, through the Office of Spent Fuel and Waste Science and Technology. Thank you to Jessica Kruichak for performing the technical review on the material in this report.

This page is intentionally left blank.

CONTENTS

LIST OF FIGURES

LIST OF TABLES

This page is intentionally left blank.

ACRONYMS

BWR	boiling water reactor
DOE	US Department of Energy
DHC	delayed hydride cracking
DPC	dual-purpose canister
EOC	end of cycle
EOL	end of life
EPRI	Electric Power Research Institute
FEP	feature, event, and process
FMDM	fuel matrix degradation model
IAEA	International Atomic Energy Agency
IFBA	integral fuel burnable absorber
INPO	Institute of Nuclear Power Operations
KAERI	Korea Atomic Energy Research Institute
NRC	US Nuclear Regulatory Commission
ORNL	Oak Ridge National Laboratory
PNNL	Pacific Northwest National Laboratory
PWR	pressurized water reactor
R&D	research and development
RIP	rod internal pressure
SCC	stress corrosion cracking
SFWST	Spent Fuel and Waste Science Technology
US	United States
WIPP	Waste Isolation Pilot Plant

This page is intentionally left blank

SPENT FUEL AND WASTE SCIENCE AND TECHNOLOGY
CLADDING DEGRADATION MODEL

1. INTRODUCTION

Cladding integrity must be reliably estimated, or bounded, in performance assessment efforts because radionuclide release from breached waste packages may be directly proportional to the fraction of cladding that is failed. Presently all repository programs make bounding assumptions of cladding barrier performance. Finland's planned repository at Onkalo assumes that water will penetrate the canister insert and fuel cladding in 1,000 years upon canister breach in their baseline scenario. In the safety analysis for Sweden's proposed repository at Forsmark "cladding is not assumed to constitute a barrier to radionuclide release from the fuel" (SKB 2011). The Canadian repository effort takes no credit for cladding. The Yucca Mountain Repository license application (DOE 2008) ultimately took no credit for cladding, that is all fuel rods were conservatively assumed to be directly exposed to in-package fluids upon waste package breach and water entry. Although early analyses concluded that cladding at Yucca Mountain would limit radionuclide releases (e.g., CRWMS M&O 2000b), the overall calculated margin of safety was sufficient to allow the total system performance assessment for the license application to conservatively neglect the additional barrier function provided by cladding (DOE 2008).

The 2019 Research and Development (R&D) Roadmap Update (Sevougian et al. 2019) identified cladding degradation as an important gap in the United States (US) Department of Energy (DOE) Spent Fuel and Waste Science and Technology (SFWST) Campaign's ongoing analyses of generic nuclear waste disposal concepts. Predicting cladding degradation behavior is challenging for generic systems studies because the behavior is sensitive to chemical conditions, especially temperature, pH, and fluoride levels, all of which are specific to the given repository setting. In addition, the prospect of direct disposal of dual-purpose canisters (DPCs) means that future performance assessment efforts may need to account for the possibility of in-package criticality events (Hardin et al. 2015). The increased temperature conditions expected for such an event (Price et al. 2019) would affect cladding degradation.

This report begins with an evaluation of cladding degradation mechanisms deemed important to assessing barrier capability. Presented in Section 2, the evaluation differs from previous similar efforts in that it accounts for the hypothetical conditions associated with direct DPC disposal, including conditions resulting from a postulated, in-package, steady-state criticality event. A total of 16 cladding degradation mechanisms are examined assuming direct disposal of DPCs in two different hypothetical repositories: a saturated repository in shale and an unsaturated repository in alluvium. The evaluation includes information from earlier studies supporting Yucca Mountain (CRWMS M&O 2000a; CRWMS M&O 2000b,d; CRWMS M&O 2001; BSC 2004a) as well as more recent work involving DPCs (Hardin et al. 2019; Price et al. 2019, 2020, 2021; Alsaed and Price 2020; Alsaed 2020). Key elements of this new evaluation include (1) an updated analysis of the impacts of localized corrosion due to evaporative concentration of salts, (2) an analysis of high temperature creep during a postulated criticality event in a saturated shale repository, (3) calculation of postulated criticality event impacts on rod internal pressure, and (4) a closer examination of Zircaloy cladding and spacer grid degradation during a postulated criticality event.

The evaluation results indicate that most of the cladding degradation mechanisms are too unlikely or the effects are too slow or too minor to be significant. However, three mechanisms—early cladding failure, general corrosion, and fluoride-enhanced corrosion—are identified for consideration as candidates to be included in a cladding degradation model. Section 3 describes the conceptual model for these mechanisms, followed by initial recommendations for cladding degradation modeling procedures accommodating the mechanisms.

This page is intentionally left blank.

2. EVALUATION OF CLADDING DEGRADATION MECHANISMS

The first step towards developing a cladding degradation model that accounts for the physical and chemical environment expected with direct DPC disposal is to evaluate the potential cladding degradation mechanisms and identify candidate mechanisms to include in the model. Section 2.1 describes the general approach for the evaluation, and Section 2.2 provides the individual evaluations for each mechanism. A summary of results, including identification of the mechanisms considered to be candidates for incorporation into a cladding degradation model, is presented in Section 2.3.

2.1 Evaluation Approach

The evaluation depends on (1) determining the repository conditions under which the evaluation is to be conducted, and (2) identifying the cladding degradation mechanisms to be evaluated. As discussed in Section 2.1.1, the repository conditions of interest are those relevant to the direct disposal of DPCs. Section 2.1.2 describes how the cladding degradation mechanisms were identified, and Section 2.1.3 addresses the evaluation limitations.

2.1.1 Repository Conditions Relevant to Direct Disposal of DPCs

Multiple studies exploring the possibility of direct disposal of DPCs have been conducted in recent years (e.g., Hardin et al. 2015, 2019; Price et al. 2019, 2020, 2021; Alsaed and Price 2020; Alsaed 2020). According to an investigation of the probability of occurrence of an in-package criticality event in DPCs during the postclosure performance period (Hardin et al. 2015), it is not clear that in-package criticality events in DPCs can be excluded from a performance assessment on the basis of probability for all geologies. As a result, the consequences of an in-package criticality event, including increased temperature conditions, must be considered in the evaluation of cladding degradation mechanisms used to support development of a cladding degradation model.

The conditions selected for the evaluation reflect the studies conducted on the effects of an in-package, steady-state criticality event in a DPC lasting for 10,000 years (e.g., Hardin et al. 2019; Price et al. 2019, 2020, 2021). The majority of the information developed thus far considers studies that rely on two geologic reference cases: a saturated shale repository and an unsaturated alluvium repository. Likewise, the evaluation focuses on these two geologic reference cases, though there may occasionally be observations made regarding hypothetical repositories in other geologies.

The geologic reference case for a hypothetical repository in saturated shale, or argillite, is illustrated in Figure 1. For this reference case, the repository is placed at a depth of 500 m, the emplacement drifts are backfilled with bentonite as a buffer (Mariner et al. 2017), and the waste package center-to-center spacing is 20 m (Hardin and Kalinina 2016).

Figure 2 depicts the hypothetical reference case for a repository in unsaturated alluvium. The repository depth is 250 m, and waste drifts are backfilled with crushed alluvium (based on Mariner et al. 2018). The drift diameter is 4.5 m, and the maximum percolation rate, corresponding to very wet conditions, is 10 mm/yr.

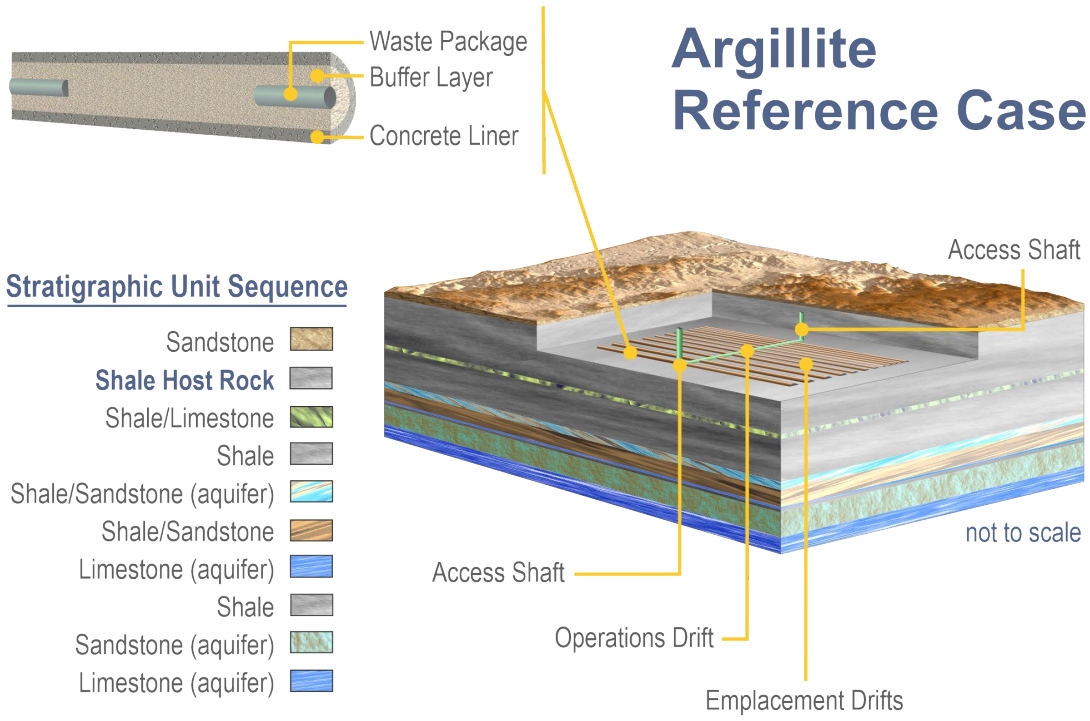

Source: Price et al. 2019, Figure 1-1.

Figure 1. Conceptual Drawing of Hypothetical Reference Case for Saturated Shale/Argillite

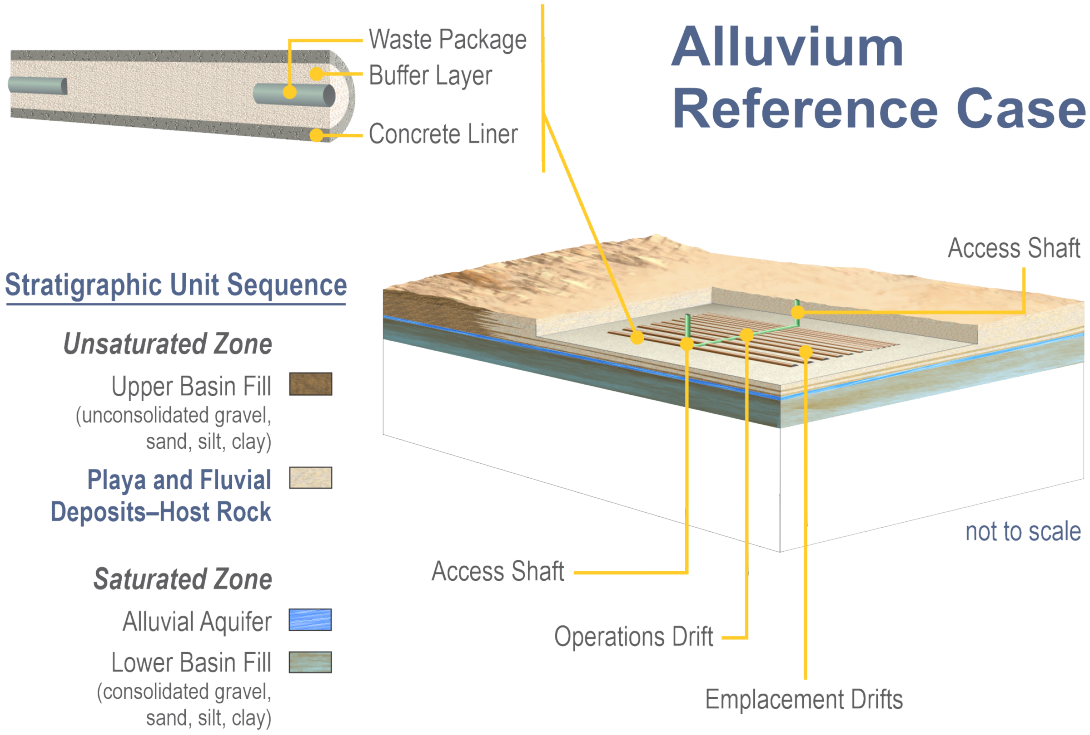

Source: Price et al. 2019, Figure 1-2.

Figure 2. Conceptual Drawing of Hypothetical Reference Case for Unsaturated Alluvium

Under nominal conditions (i.e., no criticality event) and repository time scales, cladding evolution involves multiple degradation mechanisms such as stress corrosion cracking (SCC), delayed hydride cracking (DHC), pitting, and creep. In addition, the initial state of the cladding and fuel burnup are key indicators of the potential for long-term stability after disposal. The Zircaloy used for cladding is typically coated by a durable, rapidly self-healing passivation layer of ZrO_2 that makes the cladding resistant to the degradation effects of most groundwaters, in-package fluids, and microbes in a repository environment. However, at the time of emplacement, a small percentage of the cladding may have already failed either in the reactor or during transportation or disposal operations. As-received cladding that has failed is more likely to unzip. Fuel burnup affects the amount of surface oxidation, absorbed hydrogen, fission gas production and release, rod internal pressure, and fuel pellet swelling and the corresponding free volume reduction (CRWMS M&O 2000d).

If a DPC-based waste package experiences a steady-state criticality event, the resulting increased temperatures would cause the Zircaloy to degrade much more rapidly, particularly through general corrosion. Degradation rates of Zircaloy grid spacers and guide tubes are of particular interest since they are thin, and their degradation might allow fuel rod consolidation and criticality termination. Hardin et al. (2019) noted "oxidation and localized corrosion are most appropriate for consideration in response to disposal criticality, because of elevated temperature and the potential for evaporative concentration of solutes during repeated, episodic heating events."

The expected magnitude of the increase in temperature due to a steady-state criticality event is different for the two geologic reference cases. While a steady-state criticality event in a saturated shale repository could cause temperatures to reach about 250°C, the expected peak temperatures in an unsaturated alluvium repository do not exceed 100°C (Price et al. 2020). Regardless of the reference case, the peak temperatures estimated for a steady-state criticality event are still significantly below the temperatures experienced by cladding in a pressurized water reactor (PWR) or a boiling water reactor (BWR). In a PWR, the cladding temperatures typically range from about 275°C to 315°C; the maximum cladding temperature in a BWR is about 285°C.

Besides temperature, cladding degradation is also sensitive to pH and fluoride levels. Below about 100°C, general corrosion can fail cladding only if the cladding is exposed to waters containing elevated dissolved fluoride levels (>5 ppm) at a low pH (<3.2). This form of general corrosion is referred to in this report as fluoride-enhanced corrosion. While there is a small possibility that fluoride salt levels could become evaporatively concentrated in the unsaturated alluvium repository; no such evaporative concentration of fluoride salts could happen in the saturated shale repository. In-package fluids in both repositories are expected to be near neutral, before and during a postulated criticality event (Price et al. 2020). The shale fluids would be more reducing (higher H_2 pressures), particularly at the high temperatures of a postulated criticality event because of the accelerated degradation of steel.

Further discussion of how the expected conditions (i.e., temperature, fluoride levels, and pH) for the two geologic reference cases affect the different cladding degradation mechanisms is located in Section 2.2.

2.1.2 Identification of Cladding Degradation Mechanisms through FEPs

Identification of the set of cladding degradation mechanisms to include in the evaluation began with an examination of the features, events, and processes (FEPs) analyzed for the Yucca Mountain Repository (DOE 2008). Table 1 lists 16 FEPs related to various aspects of cladding degradation.

Table 1. FEPs Addressing Cladding Degradation Mechanisms

FEP No.	FEP Title
2.1.02.11.0A	Degradation of Cladding from Waterlogged Rods
2.1.02.12.0A	Degradation of Cladding Prior to Disposal
2.1.02.13.0A	General Corrosion of Cladding
2.1.02.14.0A	Microbially Influenced Corrosion of Cladding
2.1.02.15.0A	Localized (Radiolysis Enhanced) Corrosion of Cladding
2.1.02.16.0A	Localized (Pitting) Corrosion of Cladding
2.1.02.17.0A	Localized (Crevice) Corrosion of Cladding
2.1.02.18.0A	Enhanced Corrosion of Cladding from Dissolved Silica
2.1.02.19.0A	Creep Rupture of Cladding
2.1.02.20.0A	Internal Pressurization of Cladding
2.1.02.21.0A	Stress Corrosion Cracking of Cladding
2.1.02.22.0A	Hydride Cracking of Cladding
2.1.02.23.0A	Cladding Unzipping
2.1.02.24.0A	Mechanical Impact on Cladding
2.1.02.26.0A	Diffusion-Controlled Cavity Growth in Cladding
2.1.02.27.0A	Localized (Fluoride Enhanced) Corrosion of Cladding[a]

NOTE: [a]While the mechanism in the FEP title is called "Localized (Fluoride Enhanced) Corrosion", a study by CRWMS M&O (2000a) indicates that fluoride enhancement affects general corrosion, not localized corrosion. Therefore, this report refers to the mechanism as "fluoride-enhanced corrosion" rather than maintaining the title of the FEP.

The FEPs analyses for the Yucca Mountain Repository did not include the possibility of a criticality event because such an event was excluded on the basis of low probability. However, Alsaed and Price (2020) conducted a study to investigate the FEPs relevant to DPC disposal criticality analysis. The study used the Yucca Mountain FEPs as well as additional FEPs developed in Freeze et al. (2011) as a starting point to evaluate the FEPs that could affect or be affected by an in-package criticality event. In addition, the study identified for further development additional FEPs not previously considered.

Results from Alsaed and Price (2020) show that the cladding degradation mechanisms identified in the 16 FEPs in Table 1 constitute an appropriate set of mechanisms to use for this evaluation even when considering the effects of an in-package criticality event. The study provided the following assessment of the 16 FEPs (Alsaed and Price 2020, Table 6-1):

> These FEPs could affect the evaluation of in-package criticality probability and/or consequences and they could also be affected by the consequences of a criticality event. Degradation of cladding can affect the probability of occurrence of postclosure criticality and can affect the duration of the criticality event. Once cladding degradation has resulted in a significant change in the configuration and composition of the fuel pellets and rods, the criticality event might not initiate or, if already initiated, might cease. Alternatively, preferential dissolution of neutron absorbers from the fuel could increase the probability and duration of a criticality event. The occurrence of a criticality event could damage the cladding (e.g., from a rapid transient) or enhance its corrosion rate (e.g., elevated temperatures from a quasi-steady state criticality event).

While all of the mechanisms listed in Table 1 (except FEP 2.1.02.18.0A Enhanced Corrosion of Cladding from Dissolved Silica) have been observed experimentally, not all of them are affected by repository conditions. Two of the FEPs—FEP 2.1.02.11.0A Degradation of Cladding from Waterlogged Rods and FEP 2.1.02.12.0A Degradation of Cladding Prior to Disposal—would not be affected by a postulated criticality event because they occur before disposal; however, they are included in the evaluations in Section 2.2 for completeness.

Note that, while the title of FEP 2.1.02.27.0A is "Localized (Fluoride Enhanced) Corrosion of Cladding", a study on Zircaloy corrosion by CRWMS M&O (2000) indicated that fluoride enhancement affects general corrosion, not localized corrosion. All other halides prompt pitting. Therefore, this report refers to the degradation mechanism in FEP 2.1.02.27.0A as "fluoride-enhanced corrosion" rather than maintaining the title of the FEP.

2.1.3 Evaluation Limitations

The evaluation of cladding degradation mechanisms in this report is subject to various limitations discussed below.

Focus on Steady-State Criticality Event—The conditions resulting from an in-package criticality event are limited to those pertinent to a steady-state criticality event. While the effects of a transient criticality event are being studied, the information available was not sufficient to support this evaluation.

Focus on Two Geologic Reference Cases—The studies researching the consequences of an in-package, steady-state criticality event focus on the saturated shale repository and the unsaturated alluvium repository. Accordingly, these two geologic reference cases are also the focus of this evaluation. However, cladding degradation behavior is sensitive to temperature, fluoride levels, and pH, all of which are specific to the given repository geologic setting. While there may occasionally be some observations about other geologic settings, this evaluation does not formally include geologies other than those represented in the two reference cases.

Focus on PWR Cladding (Zircaloy-4)—The evalution focuses on PWR cladding rather than BWR cladding. BWR cladding is thicker than PWR cladding (813 versus 570 μm), has lower burnup, and experiences less hoop stress due to a significantly lower initial helium rod backfill pressure. However, the evolution in BWR assembly design from a typical 8×8 assembly to the now-prevalent 10×10 assembly design and the introduction of 11×11 designs result in cladding dimensions (especially the cladding thickness of BWR rods) approaching the dimensions of PWR rods. While the rod internal pressures for BWR cladding are much lower than for PWR cladding, BWR cladding tends to corrode more than PWR cladding because of the aggressive nature of steam. For this review, the behavior of PWR cladding is assumed to bound that of BWR cladding; however, this assumption should be investigated further for confirmation as it may not hold for a few mechanisms such as general corrosion.

Zircaloy-2 was and still is used for BWR cladding. Zircaloy-4 was the primary alloy used for PWR cladding until the late 1990s and early 2000s. Zircaloy-4 contains less nickel and more iron than Zircaloy-2. With the push to achieve higher burnups, the industry developed zirconium-based alloys that

are more resistant to oxidation and hydrogen pickup, two of the main factors that limit the burnup for Zircaloy-4 clad fuel. Framatome introduced M5® cladding, a fully recrystallized zirconium-niobium alloy with no tin and controlled oxygen, iron, and sulfur content in the mid-1990s. Westinghouse introduced ZIRLO®, which, though also a stress-relief annealed zirconium-niobium alloy, still contains some tin. By 2010, full core loads of Optimized ZIRLO™, which is partially recrystallized and has optimized tin content, were used for PWRs. These newer alloys have significantly less oxidation and hydrogen pickup during irradiation in a reactor (Figure 3) and have superior creep and growth performance relative to Zircaloy-4. The review in this report does not consider the effects of newer cladding alloys. Approximately 1%–2% of the fuel slated for Yucca Mountain was expected to have stainless steel, not Zircaloy, cladding. At Yucca Mountain, the stainless-steel cladding was assumed to be failed before disposal and to provide no barrier function.

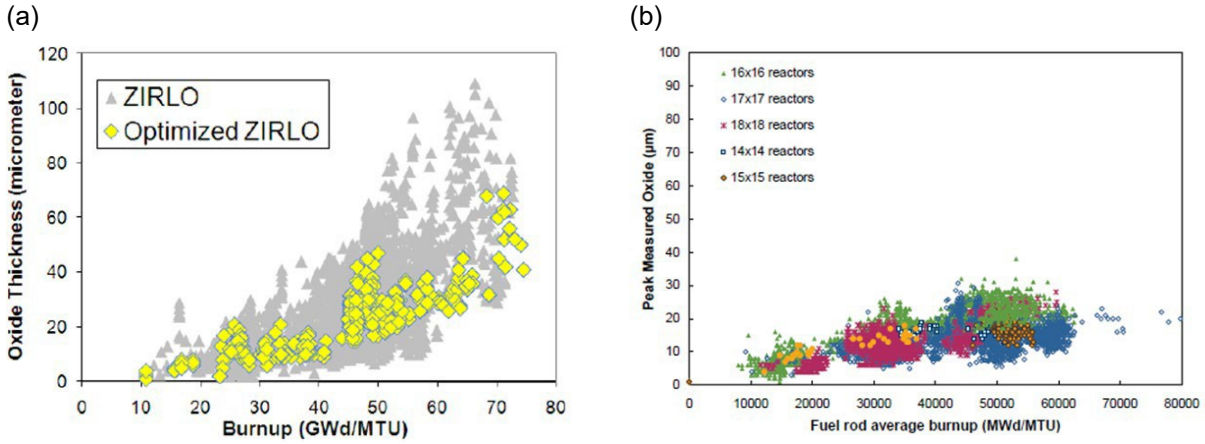

Source: (a) Pan et al. 2013; (b) Mardon et al. 2010.

Figure 3. Oxide Layer Thickness as a Function of Burnup for (a) ZIRLO® and Optimized ZIRLO™ and (b) M5® Cladding

2.2 Individual Evaluations of Cladding Degradation Mechanisms

The subsections below present the individual evaluations for each of the 16 cladding degradation mechanisms identified in Table 1. The evaluation approach is presented in Section 2.1, including the process used to select the mechanisms (Section 2.1.2).

2.2.1 Degradation of Cladding from Waterlogged Rods

CRWMS M&O (2000d) discounted any effect of spent pool storage on cladding condition citing reviews by the International Atomic Energy Agency (IAEA 1988) and DOE (Johnson 1977). CRWMS M&O (2000d) concluded that "fuel failure or degradation is not expected during pool storage, and the fuel failure rates observed from reactor operation are appropriate for the cladding degradation analysis." Typically, spent fuel pools are required to have temperatures ≤60°C, resulting in temperatures being maintained between 25°C and 35°C. Water purity is also maintained. The low temperatures and water purity contribute to very low cladding degradation rates in US spent fuel pools.

2.2.2 Degradation of Cladding Prior to Disposal

CRWMS M&O (2000b) calculated the as-received failure rate of rods expected at Yucca Mountain to be 0.0155%–1.285% (median = 0.0948%). This range represents failure due to reactor operations + pool

storage + dry storage + handling/consolidation + transport. A broadly parallel analysis done by S. Cohen & Associates (1999) corroborated the results of CRWMS M&O (2000b) with a similar clad failure distribution, 0.01%–1% (SNL 2007a); a median failure rate of 0.1% was chosen for use at Yucca Mountain (SNL 2007a). Table 2 presents the rod failure rates estimated for the different individual origins of early cladding failure.

Table 2. Fuel Failure Sources

Fuel Service Period	Rod Failure Rate (%)
In-Service	<0.05
Pool Storage	0
Dry Storage	0.03
Consolidation	0.005
Other Handling	0.0003
Total	**<0.1**

Reactor operations and dry storage cause the bulk of cladding damage, though the total amount is small. It was initially thought that creep would occur at the high temperatures of dry storage. The US Nuclear Regulatory Commission (NRC) recently found that, while thermal creep during the first 60 years of dry storage is credible, "…due to the high creep capacity of zirconium-based alloys, thermal creep is not expected to result in cladding failures and reconfiguration of the fuel" (NRC 2019, Section 3.6.1.3). Similarly, the NRC concluded that "the low temperature (athermal) creep mechanism is not considered credible, even for the unlikely scenario where fuel reaches room temperature during the 60-year timeframe" (NRC 2019, Section 3.6.1.4).

CRWMS M&O (2000b) estimated dry storage to cause 0.045% of failures and transportation to cause 0.01% of failures. Figure 4 shows the trend in fuel failures in the US between 1980 and 2007 (EPRI 2008). In 2006, the Institute of Nuclear Power Operations (INPO) set a goal to achieve zero fuel failures by 2010. While this goal has not yet been achieved, the failure rate continues to decrease. Recent multilaboratory testing involved three 17×17 PWR surrogate assemblies shipped from dry storage sequentially by truck, local ship, ocean-going ship, and rail from Spain to the center of the US. This testing confirmed that transportation has a small effect on fuel. The accumulated damage fraction in all cases was below 1×10^{-10}. The maximum strain observed during the tests resulted in stresses that were far below cladding yield limits (Kalinina et al. 2019). Thus, the failure rates of CRWMS M&O (2000b) and S. Cohen & Associates (1999) should be considered as an upper bound with fewer failures for more modern fuels.

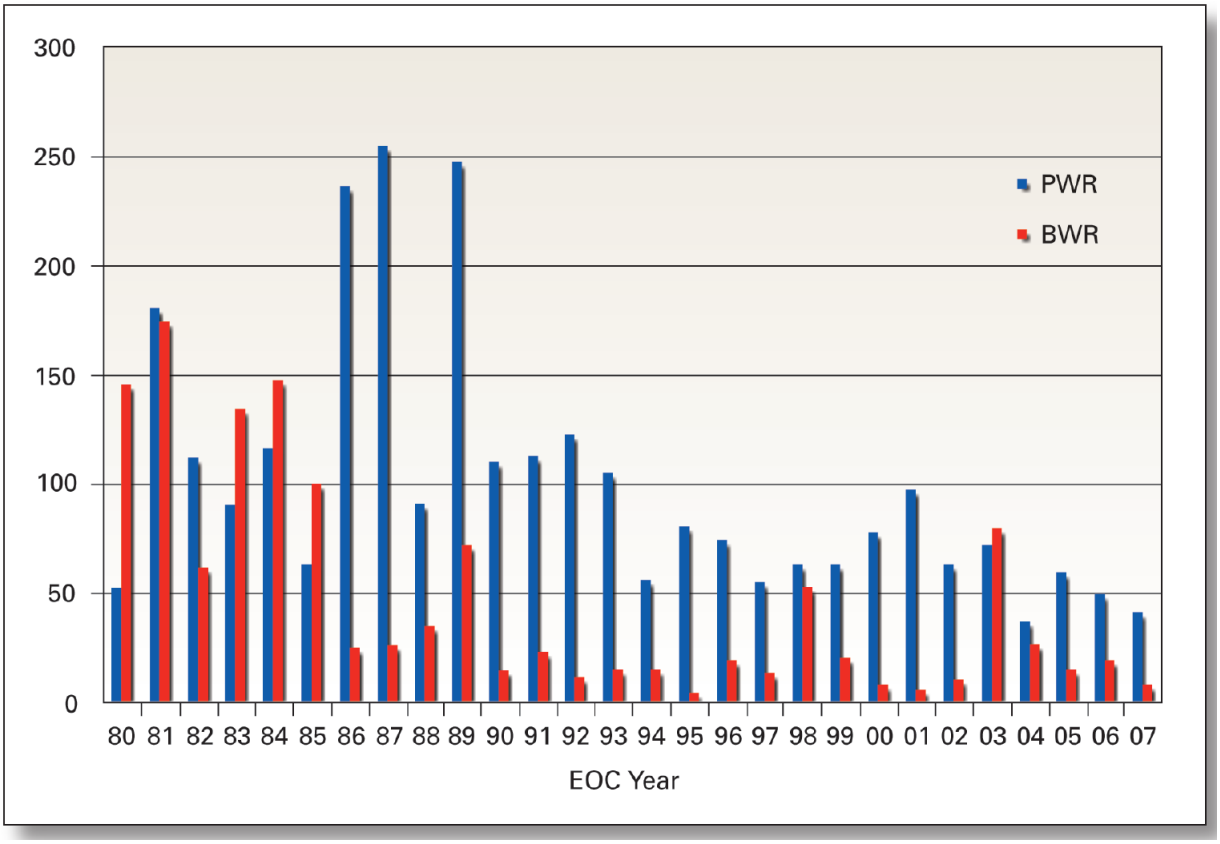

NOTE: BWR = boiling water reactor
EOC = end of cycle
PWR = pressurized water reactor

Source: ERPI 2008.

Figure 4. Fuel Failure Rates Trending Downward

2.2.3 General Corrosion of Cladding

General corrosion (oxidation) of Zircaloy is described by Equation 1:

$$Zr + 2H_2O \rightarrow ZrO_2 + 2H_2 \qquad \textit{Equation 1}$$

This reaction proceeds in three steps: (1) an early (high rate) pretransition regime during which the surface film grows by a cubic rate law, (2) a transition stage, and (3) a linear post-transition kinetic regime, which is the regime most relevant to a repository (Hillner et al. 1998). Oxygen diffusion through the passivating ZrO_2 surface layer is believed to be the rate-limiting step (Hillner et al. 1998).

The kinetics of the post-transition regime was originally described by the following rate expression (Hillner 1977):

$$\Delta W = 1.12 \times 10^{8} \exp\left[\frac{-12{,}529}{T}\right] \times t \qquad \textit{Equation 2}$$

where ΔW = ZrO_2 weight gain (mg/dm^2), T = absolute temperature (K), and t = exposure time (days).

Subsequent work (Hillner et al. 1998) indicates that post-transition corrosion accelerates after a certain point. Thus, corrosion can be described by two linear rate laws, with the second rate law expressed as

$$\Delta W = 3.47 \times 10^{7} \exp\left[\frac{-11{,}452}{T}\right] \times t \qquad \textit{Equation 3}$$

Because Equation 3 is considered to be the rate law most relevant to repository conditions, it has been used to predict general corrosion of Zircaloy in a repository setting (Hillner et al. 1998). Note that Equation 3 is also commonly referred to using Hillner's name (e.g., the Hillner equation, Hillner rate law, or Hillner general corrosion rate law). The rates used to develop Equation 3 were generally measured in near-neutral solutions. As such, Equation 3 can be applied to this evaluation because the in-package pHs for DPCs are expected to remain near neutral as well (Price et al. 2020).

Degradation rates calculated with Equation 3 may need to be modified by a multiplier to account for irradiation-induced acceleration to general corrosion. Irradiated Zircaloy degrades 2–20 times faster than nonirradiated Zircaloy (e.g., IAEA 1998, Figure 8.6) driven by radiation damage to both the passive surface layer and the underlying metal (Hillner et al. 1998). Equation 3 is based on out-of-reactor autoclave experiments, and it must be multiplied by at least a factor of 2 (Hillner et al. 1998) to describe Zircaloy corrosion in a repository undergoing a postulated criticality event. That said, there is considerable uncertainty in the underlying mechanism(s) of irradiation-induced acceleration of cladding degradation (IAEA 1998, Section 9.2). Of relevance to saturated repositories is the observation that high hydrogen levels appear to greatly reduce the irradiation effect (IAEA 1998, p. 223). Annealing of rate-accelerating irradiation damage also occurs, particularly at high temperatures. Hillner et al. (1998) noted that cladding degradation rates in a repository setting might be higher than autoclave-measured rates (and rates predicted with Equation 3) because of irradiation in the reactor before disposal. Though noting the actual effect would probably be less, Hillner et al. (1998) conservatively assumed a factor of 2 irradiation acceleration. For the calculation of Zircaloy failure times in the conceptual model description in Section 3.1, the irradiation multiplier of 2 is applied with somewhat less conservatism because a postulated criticality event itself might cause irradiation damage to the cladding.

Similar work examining oxidation rates of the newer cladding alloys (M5®, ZIRLO®, and Optimized ZIRLO™) and the new accident-tolerant designs with a thin coating of chromium on the cladding outer diameter under repository conditions has not been performed. However, given their resistance to oxidation under the high temperatures experienced in reactor operations (Figure 3), the newer alloys and accident-tolerant designs are expected to have oxidation rates under repository conditions that are significantly less than oxidation rates for Zircaloy-4.

Because of the strong dependence on temperature, general corrosion has more significance for the saturated shale repository than for the unsaturated alluvium repository. As described in Section 2.1.1, the upper bound on the temperature reached by a breached waste package experiencing a steady-state criticality event for 10,000 years in a saturated shale repository is about 250°C (Price et al. 2020). In contrast, the expected peak temperatures due to the same in-package, steady-state criticality event in an unsaturated alluvium repository are not expected to exceed 100°C (Price et al. 2020). For illustration purposes, consider these temperatures in light of following simple application of Equation 3 (without the irradiation multiplier). Given that 378 mg/dm^2 of weight gain =1 mil of oxide growth = 0.66 mil of metal

consumed, Equation 3 predicts Zircaloy general corrosion rates of 8×10^{-9} mil/yr (2×10^{-7} μm/yr) at 50°C, 9×10^{-6} mil/yr (3×10^{-4} μm/yr) at 150°C, and 7×10^{-3} mil/yr (0.18 μm/yr) at 250°C. Using these predicted rates and a typical cladding thickness of 22.5 mil, general corrosion at 250°C would dissolve cladding completely in about 3,200 years (well within the 10,000-year time span assumed for the duration of the steady-state criticality event). At 150°C, cladding would be completely dissolved in 2.5 million years. Even if the irradiation multiplier is applied, cladding degradation due to general corrosion would still be neglible at lower temperatures.

There is one exception to the idea that temperatures must be elevated for general corrosion to be significant. General corrosion can compromise cladding even at low temperatures if high fluoride (>5 ppm), low pH (<3.2) solutions contact cladding inside a breached waste package for a sufficient period of time (e.g., CRWMS M&O 2000). This form of general corrosion, referred to in this report as fluoride-enhanced corrosion, is evaluated separately in Section 2.2.16.

2.2.4 Microbially Influenced Corrosion of Cladding

Microbially induced corrosion of cladding is unlikely because Zircaloy is notably resistant to acid attack, particularly weak acids such as those produced by microbes (Hillner et al. 1998). Zircaloy is unaffected by sulfate-reducing bacteria (McNeil and Odom 1994). Microbiologically induced corrosion, crevice corrosion, and pitting have not been observed in reactor operation or pool storage (CRWMS M&O 2000d). If anything, the high temperatures of a postulated criticality event would tend to inhibit microbial activity. Otherwise, no criticality effect is expected.

2.2.5 Localized (Radiation-Enhanced) Corrosion of Cladding

Radiolytic production of nitric acid (unsaturated alluvium repository) or hydrogen peroxide (unsaturated alluvium and saturated shale repositories) is unlikely to accelerate cladding corrosion in a repository environment because zirconium is inert in hydrogen peroxide (Yau and Webster 1987) and in up to 65% nitric acid (BSC 2004a). In the unsaturated alluvium repository, pH shifts from nitric acid production will be prevented by pH-buffering dissolution of corrosion products (Price et al. 2020). Radiation-enhancement of general corrosion by a postulated criticality event is discussed in Section 2.2.3.

2.2.6 Localized (Pitting) Corrosion of Cladding

Clad pitting requires the following: (1) low pH (pH<2.5), (2) sufficiently oxidizing ions, most notably Fe^{3+}, (3) high concentrations of halides, particularly chloride >1 mM, and (4) the presence of electrochemically conducive surface contaminants (e.g., Fahey et al. 1997) or the absence of the passivating oxide surface layer (BSC 2004a). In-package fluids in a saturated shale or unsaturated alluvium repository are expected to have near-neutral pH levels, before and during a postulated criticality event (Price et al. 2020) even after being evaporatively concentrated (unsaturated alluvium repository). Growth of ferric (hydr)oxide minerals such as hematite or goethite will limit Fe^{3+} to sub-ppm levels under the oxidizing conditions of the unsaturated alluvium repository; reduction of Fe^{3+} to Fe^{2+} will limit Fe^{3+} to sub-ppm levels in the saturated shale repository. For comparison, CRWMS M&O (2000a) suggested that at least 50 ppm Fe^{3+} is needed to accelerate Zircaloy corrosion. The presence of nonconductive, thick, oxide layers on cladding should mitigate the potential for pitting by electrochemically conductive surface contaminants, as would pickling (CRWMS M&O 2000a). In short, the enabling conditions for pitting will not exist for pitting corrosion in a repository, though the oxide thickness of newer alloys may make them more susceptible. Moreover, a postulated criticality event would not alter this absence of enabling conditions.

2.2.7 Localized (Crevice) Corrosion of Cladding

Evidence indicates Zircaloy will not corrode in a repository through crevice corrosion (e.g., Yau and Webster 1987; Fraker 1989; BSC 2004a). CRWMS M&O (2000a) notes, "Zirconium is one of the most crevice corrosion resistant materials. For example, it is not subject to crevice corrosion even under such adverse conditions as low-pH chloride solutions or wet chlorine gas." No effect of a postulated criticality event is expected to change this observation.

2.2.8 Enhanced Corrosion of Cladding from Dissolved Silica

There is no evidence supporting the occurrence of silica-enhanced corrosion of cladding, but some indirect evidence (BSC 2004a) exists suggesting that silica has no effect on cladding corrosion. No effect of a postulated criticality event is expected to change this observation.

2.2.9 Creep Rupture of Cladding

Creep rupture of cladding is more likely to be a factor during dry storage or the first several hundred years after disposal because of the higher temperatures involved compared to the cooler temperatures that occur later in the postclosure period. Unirradiated Zircaloy may sustain greater than 10% strain without rupture, while high burnup fuel may fail at 4% strain (Hardin et al. 2019). Tensile stress magnitude in the Zircaloy (hoop stress) of less than 90 MPa has been shown to substantially reduce the rate of creep strain accumulation (Hardin et al. 2019). Internal pressurization of rods by gas production causes tensile stresses leading to creep, but only at relatively high temperatures (>300°C). Repository temperatures will be too low for creep rupture of cladding (BSC 2004a), even should a temperature increase from a criticality event occur. Creep rupture was thought to be a significant degradation mechanism during dry storage where temperatures are higher, but recent work (NRC 2019; EPRI 2020) has shown that (1) hoop stresses are significantly lower than originally hypothesized and (2) thermal creep is not expected to result in cladding failures and reconfiguration of the fuel during dry storage. Unlike most other cladding failure mechanisms, creep rupture does not require waste package breach and contact with fluids. Key to creep rupture is the gas pressure internal to the rod, which is a function of the amount of gas and the available void volume. The amount of gas depends on the gas initially present in the rod plus any added fission product gasses, which depend upon fuel burnup and power in the reactor (Section 2.10). The internal void volume is made up of fuel–cladding gaps, pellet–pellet gaps, and plenum volume (e.g., Hardin et al. 2019). Also, the fuel pellets swell slightly with burnup.

Although independent of increased gas pressure, cladding creep is sensitive to thinning due to corrosion (oxide layer formation) and cladding embrittlement. Cladding that has been thinned or embrittled will rupture at lower total creep strains. Cladding creep may result in rupture if the total creep strain exceeds a threshold of about 6%. As mentioned above, unirradiated Zircaloy may sustain greater than 10% strain without rupture, while high burnup fuel may fail at 4% strain (Hardin et al. 2019). Irradiation embrittlement causes creep rupture where burnup is greatest—near the center of the rod.

Cladding creep failure was estimated for Yucca Mountain (CRWMS M&O 2000b) by comparing predicted strain, using Murty correlations measured between cladding temperature history and observed creep strain, against probabilistic estimates of the critical strain needed for cladding failure. Murty correlations sum together expressions that account for high stress glide creep and low stress Coble creep (Henningson et al. 1998) in unirradiated cladding at a specific time, t (hours). Murty correlations were chosen over Matsuo correlations because they specifically consider Coble creep, a mechanism likely to be observed in the relatively low temperatures of a repository. The parameter ε is dimensionless and must be multiplied by 100 to calculate % creep:

$$\varepsilon = \varepsilon_{glide} + \varepsilon_{glide} \qquad \textit{Equation 4}$$

$$\varepsilon_{glide} = \dot{\varepsilon}_{glide} t + \frac{K \varepsilon_T \dot{\varepsilon}_{glide} t}{\varepsilon_T + K t \dot{\varepsilon}_{glide}} \qquad \textit{Equation 5}$$

$$\dot{\varepsilon}_{glide} = 4.97 \times 10^6 \; exp\left[\frac{-31{,}200}{T}\right] \frac{E}{T} \left[\sinh\left(807 \frac{\sigma}{E}\right)\right]^3 \qquad \textit{Equation 6}$$

$$\varepsilon_{Coble} = 8.83 \; exp\left[\frac{-2{,}100}{T}\right] \frac{\sigma}{T} \; t \qquad \textit{Equation 7}$$

where

$\varepsilon_T = 0.008$

$K = 10$

$E = (1.148 \times 10^5 - 59.9T) \times 10^6$

$T =$ temperature (K)

$\sigma =$ stress (Pa)

The Murty equations above were modified to account for lower clad creep that is observed in irradiated clad at high temperatures with the following equation (CRWMS M&O 2000c):

$$MM(\%) = 0.233 \times M(\%)^{0.488} \qquad \textit{Equation 8}$$

where *M* is the % creep strain predicted by the unmodified Murty equations above for unirradiated clad and *MM* is the % creep strain predicted for irradiated clad.

Accumulated creep at time t_i is calculated with the following equation over assumed clad temperature-time segments (CRWMS M&O 2000b).

$$\varepsilon(t_i) = \varepsilon(T_{i-1}, t_{i-1}) + [\varepsilon(T_i, t_i) - \varepsilon(T_i, t_{i-1})] \qquad \textit{Equation 9}$$

A conservative creep-failure relationship was approximated by CRWMS M&O (2000b) from irradiated cladding failure tests as

$$Fs = 14.4 - 135P;\ 0.0 < P \leq 0.06 \qquad \textit{Equation 10}$$

$$Fs = 6.77 - 7.81P;\ 0.06 \leq P \leq 0.5 \qquad \textit{Equation 11}$$

$$Fs = 5.33 - 4.93P:\ 0.5 \leq P \leq 1.0 \qquad \textit{Equation 12}$$

where Fs is the strain failure limit (%) and P is a random probability between 0 and 1.

The approach of CRWMS M&O (2000b) when applied to the higher temperature of a hypothetical, saturated shale repository undergoing a postulated criticality event estimates an additional 0.191% creep strain, at 250°C for 10,000 years for cladding under a (relatively high) stress of 100 MPa. The additional creep of 0.191% is very small compared to the failure probability relations noted above, suggesting that a postulated criticality event will have little tangible impact on creep failure of cladding in a saturated shale repository. The additional creep strain caused by a much lower temperature (<100°C) postulated criticality event in a hypothetical, unsaturated alluvium repository is orders of magnitude less than that for a saturated shale repository, hence negligible.

2.2.10 Internal Pressurization of Cladding

A relatively high rod internal pressure favors failure from cladding creep, hydride reorientation, DHC, and SCC (CRWMS M&O 2000d). Rod pressurization, which sets the cladding hoop stress, is a function of the available volume; the temperature; the initial helium fill pressure (assumed for Yucca Mountain to be uniformly distributed between 2 and 3.5 MPa); and the production rates of gas phase fission products (primarily isotopes of Xe and Kr), fission gas release from the fuel matrix, and helium production from alpha decay. Once rods are removed from the reactor, fission product accumulation is sharply limited, but helium will continue to accumulate.

CRWMS M&O (2000d) developed a numerical expression for rod internal pressure over time by first building correlations between the following: fuel burnup and fission product release; temperature, time, and helium pressure; and burnup and fuel rod volume change. CRWMS M&O (2000d) calculated a mean rod internal pressure of 5 MPa at 100 years, 27°C, for a fuel burnup of 50 MWd/kgU; for a fuel burnup of 75 MWd/kgU the calculated internal pressure was 10 MPa. CRWMS M&O (2000d) set the rod plenum failure pressure to be the reactor system pressure, ~15 MPa at 320°C and ~7.5 MPa at 27°C. A failure pressure of 13 MPa at 250°C is used in the analysis below for the shale postulated criticality condition. CRWMS M&O (2000d) estimated that ~4.5% of the fuel rods going to Yucca Mountain approached the reactor system pressure. Figure 5 shows the end-of-life, rod internal pressure at room temperature (25°C) from the international, publicly available database, including work recently performed on the high burnup sibling pins at both Oak Ridge National Laboratory and Pacific Northwest National Laboratory. In the US, the NRC currently limits the peak rod-average burnup to 62 MWd/kgU. Note that the mean for burnups below the US limit of 62 MWd/kgU is approximately 4 MPa, which results in a pressure of only 9 MPa for a uniform temperature of 400°C. One of the major reasons that rod internal pressures, and thus hoop stresses, are significantly lower than previously estimated is that the initial fill pressure of helium has been decreasing in newer designs.

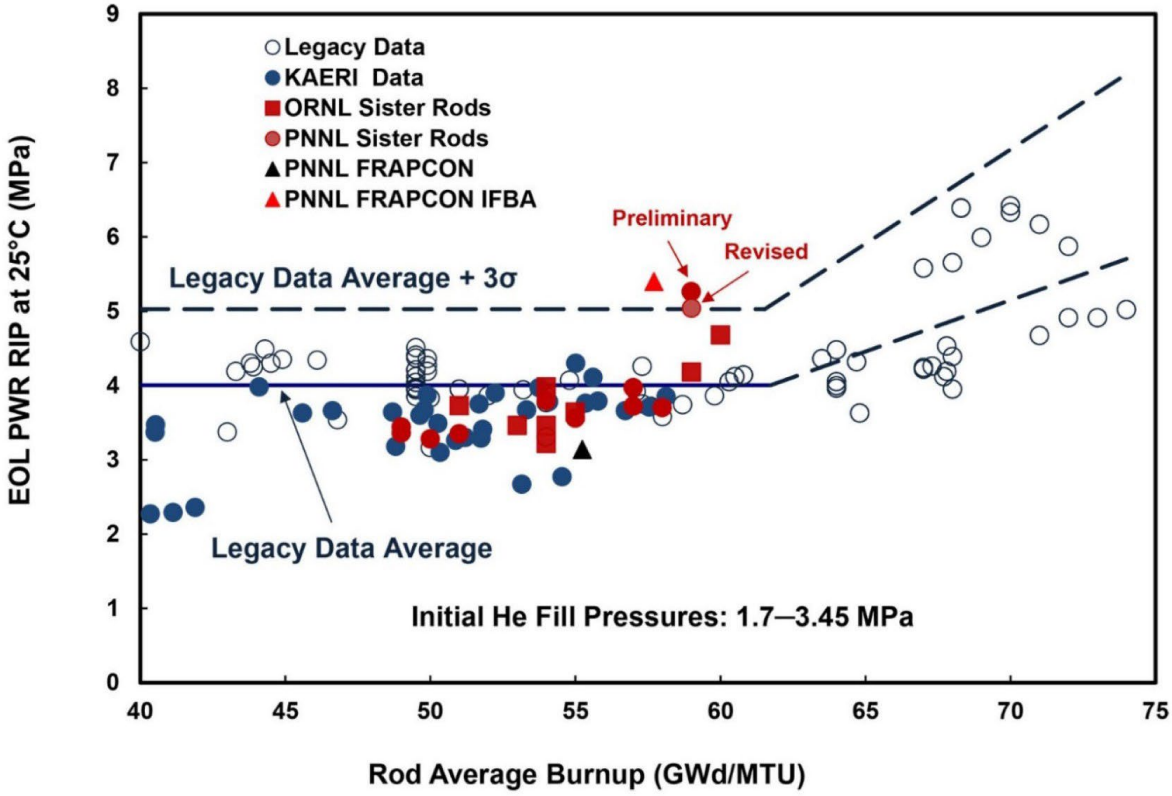

NOTE: EOL = end of life
IFBA = integral fuel burnable absorber
KAERI = Korea Atomic Energy Research Institute
ORNL = Oak Ridge National Laboratory
PNNL = Pacific Northwest National Laboratory
PWR = pressurized water reactor
RIP = rod internal pressure

Source: Billone and Burtseva 2020.

Figure 5. End-of-Life Rod Internal Pressure Data Extrapolated to 25°C

Fission gas production is linearly proportional to the fuel burnup, 31 cm^3/MWd at standard temperature and pressure. Decay of fission product gases over the lifetime of a repository will be small (CRWMS M&O 2000d, p. 25) as most of these gases are stable (except for ^{85}Kr with a 10-year half life). The majority of the fission gases are not released, but instead remain in the fuel matrix. While fission product release from the matrix depends in part on burnup, the power history of the fuel is the primary factor (CRWMS M&O 2000d). A postulated criticality event would cause a resurgence in fission product accumulation and would probably minimally increase their release from the fuel matrix because of increased fission product diffusion at high temperatures (saturated shale repository). The reason is that, during reactor operations with very high power relative to the power estimated for postclosure postulated criticality scenarios, the fuel pellet centerline temperatures range between 800°C and 1,200°C with fuel pellet surface temperatures close to that of the cladding and coolant, ~300°C. It is this large temperature gradient, especially in high burnup fuels, that drives the small amount of fission gas release. An Electric

Power Research Institute (EPRI) study (EPRI 2013) found that "the weak dependence of the number of moles…may be indicative of the fact that the contribution of moles from fission gas release is small compared to the initial fill gas for the general population of fuel rods."

The much lower powers during a postclosure postulated criticality event will have a negligible effect on fission gas release and rod pressurization. For example, a steady-state criticality event at a power level of 4 kW for 10,000 years would result in an additional ~1 MWd/kgU average burnup in a typical DPC. A steady-state criticality event at a power level of 400 W lasting 10,000 years would result in an additional ~0.1 MWd/kgU average burnup in a typical DPC (Price et al. 2019). The added burnup from these postulated criticality events is less than 1% of the average burnup assumed for Yucca Mountain fuel (~45 MWd/kgU); thus, the estimated criticality-related burnup would result in an insignificant increase in fission gas pressure. Calculations done at Oak Ridge National Laboratory for a 2.1 kW criticality event for 15,000 years indicate a minor (<1%) increase in fission product Kr and Xe gasses from the baseline, noncritical case. The criticality temperature shift from 50°C to about 250°C (saturated shale repository) alone would increase the rod pressure by ~60%, a much larger increase.

Johnson and Gilbert (1983) calculated He pressure buildup from alpha decay for a fuel with 36 MWd/kgU burnup showing that this process could become a significant contributor (He pressure >1 MPa) to total rod internal pressure in a repository after ~1,000 years. Independent of time, the calculated He pressure becomes greater at higher temperature as well. Again, a criticality-driven jump in temperature alone from 50°C to about 250°C would amount to a 60% increase in rod internal pressure. In short, the primary effect of a postulated criticality event will be to increase rod pressure by raising temperature. However, as demonstrated in Figure 5, even assuming the average +3σ value of 5 MPa at 25°C, the pressure at 250°C would still only be less than 9 MPa.

2.2.11 Stress Corrosion Cracking of Cladding

SCC occurs by cracks propagating in materials subjected to a combination of concentrated local stress and aggressive chemicals concentrating at crack tips (Fraker 1989; CRWMS M&O 2000b). Initially for Yucca Mountain, any rod with a hoop stress calculated to be greater than 180 MPa (twice the cladding creep threshold of 90 MPa) was assumed to fail from SCC (CRWMS M&O 2000b) based on the results of Tasooji et al. (1984). Pescatore et al. (1990) argued for an even higher SCC clad stress threshold of 200 MPa, and the NRC (2019) states "…analysis indicates that at least 240 MPa of hoop stresses are needed to induce SCC for both Zircaloy-2 and Zircaloy-4." CRWMS M&O (2000b) calculated hoop stress from predicted internal pressures (Section 2.2.10), clad thinning by corrosion, and clad crack distribution. If the requisite stress existed, SCC could be driven by Cs and I (fuel-side SCC) or chloride (water-side SCC). Rapid repassivation tends to protect Zircaloy from SCC. Zirconium and its alloys are resistant to SCC in seawater, most aqueous environments, and some sulfate and nitrate solutions (e.g., Fraker 1989).

Hardin et al. (2019) noted that "[h]oop stress is less than 90 MPa for the great majority of spent fuel cladding even at elevated temperature up to 350°C, and virtually all cladding at lower temperatures". Because the stresses required for SCC "are higher than those expected to predominate in actual cladding, even at elevated temperature … SCC is unlikely if temperature is limited (as would be the case for criticality events in an unsaturated repository with maximum temperature limited by boiling) or there is a constant supply of diluent ground water (saturated repository)" (Hardin et al. 2019).

2.2.12 Hydride Cracking of Cladding

During DHC, hydrides slowly form at a crack tip causing the crack to propagate. DHC requires an incipient crack or defect from manufacturing or irradiation, hydride at the crack tip, and sufficient stress to propagate the crack (e.g., BSC 2004a). Hydride, existing as a separate Zr hydride phase or solid solution, is formed by hydrogen existing as an impurity in the Zircaloy or produced from, for example, steel corrosion. Recall that, although hydrogen will be particularly abundant under the reducing

conditions of a saturated shale repository, hydrogen generated from corrosion of waste package internals is not expected to penetrate the ZrO_2 surface layer on the cladding (BSC 2004a). Zr hydride flakes are brittle and allow more rapid fracture propagation. Countering DHC is the general resilience of the Zircaloy oxide surface layer, which persists as long as water is available.

In theory, hydrogen transfer to cladding might also occur upon galvanic corrosion of basket steels in contact with Zircaloy. The process requires sustained, intimate, metal–metal contact with high contact pressures. Even then, the process is transient because corrosion breaks the metal–Zircaloy contact (BSC 2004a). DHC was screened out at Yucca Mountain (in part) because hydrogen was determined to be unlikely to penetrate the passive ZrO_2 surface coating of the cladding. Cladding stresses were also calculated to be too low for DHC to occur. Stress intensity factors are calculated to have a mean of 0.47 $MPa \cdot m^{0.5}$ (range 0.002–2.7 $MPa \cdot m^{0.5}$), which is below the threshold stress intensity factors ranging from 5 to 12 $MPa \cdot m^{0.5}$ (CRWMS M&O 2000b; BSC 2004a). A recent evaluation by EPRI (EPRI 2020) found that over a range of realistic hoop stresses, the critical crack size to sustain DHC is unrealistically large, often greater than the cladding wall thickness. Hydride reorientation, which facilitates crack propagation, requires high thermal gradients and high stress, neither of which is expected in the repository environment (BSC 2004a). As noted by Hardin et al. (2019), "[d]elayed hydride cracking has been analyzed in terms of stress intensity and found to be unlikely even at elevated temperature, so that only a small fraction of fuel (0.01%) could be affected." A postulated criticality event is therefore expected to have no effect.

2.2.13 Cladding Unzipping

Clad unzipping occurs when oxidation of exposed fuel in contact with water causes an autocatalytic peeling of the clad because of formation of oxidized uranium phases having a higher volume than the fuel (UO_2) itself, e.g., $2H_2O + UO_2 + 1/2O_2 \rightarrow UO_3{:}2H_2O_{Schoepite}$; $\Delta Volume = V_{Schoepite} - V_{UO2} = 66.70 - 24.62 = 42.08\ cm^3$. Unzipping does not occur when fuel dissolves nonoxidatively under completely reducing conditions (E_H<~100 mV at pH 7 [Jerden et al. 2015, Figure 1]) because a higher volume alteration phase is not formed, e.g., $2H_2O + UO_2 \rightarrow U(OH)_4^{aq}$. Oxidative dissolution of UO_2 is relatively rapid (1–10 g/m^2day [Jerden et al. 2020]), though fuel degradation likely decreases sharply with burnup. Under completely reducing conditions, nonoxidative UO_2 dissolution is much slower (~0.001 g/m^2day [Jerden et al. 2020]).

In between oxidizing and reducing conditions (E_H>~100 mV at pH 7 [Jerden et al. 2015, Figure 1]), electron donors and acceptors are both present, which is the most complex situation for fuel dissolution. The Fuel Matrix Degradation Model (FMDM) of Jerden and co-workers (e.g., Jerden et al. 2015; Jerden et al. 2020) is designed to predict fuel degradation rates under these conditions. FMDM is a mixed potential model that simultaneously accounts for alpha radiolysis and radiolytic production of oxidants as a function fuel burnup, accumulation of alteration phases at the spent fuel surface, H_2 production by corroding steels and Zircaloy, and electron transfer reactions occurring at/near the spent fuel surface and in the bulk solution (e.g., Jerden et al. 2015). A key feature of the FMDM is its ability to capture the inhibitory effect of dissolved H_2 on fuel degradation rates (e.g., Carbol et al. 2005; Shoesmith 2013). Experimental validation of the FMDM is ongoing.

A postulated criticality event in a saturated shale repository is likely to indirectly accelerate H_2 production from steel and Zircaloy corrosion because of the rise in temperature. Radiolytic production of H_2O_2 would be directly increased by the criticality event itself, but so would production of radicals that react with H_2O_2. The difference between H_2 production and H_2O_2 production and reaction determines whether oxidative fuel degradation, and unzipping, are inhibited. An unsaturated alluvium repository might maintain the potential for unzipping because there would be renewed H_2O_2 production from radiolysis, but less of a temperature-driven increase in H_2 production than in the higher temperature shale criticality case.

Unzipping, should it occur, is a two-step process: incubation at the site of fuel exposure, followed by splitting away from the fuel exposure site (Einziger and Strain 1986). Hardin et al. (2019) examined clad unzipping under a high temperature postulated criticality event and noted that:

- The time to splitting after perforation would be a few weeks at high temperature (283°C) but more than a million years at 100°C.
- For splitting to occur at a rate significant to repository performance, elevated temperature (>100°C) is required.

Given these observations from Hardin et al. (2019), two end-member scenarios exist for late waste package breach after the thermal period:

- In the oxidative, unsaturated alluvium repository with and without a criticality event, incubation and splitting would occur at rates so low as to be insignificant because temperatures would not exceed 100°C.
- In a highly reducing, saturated shale repository with or without a criticality event, splitting could not occur because of the absence of oxidative fuel dissolution.

Early waste package breach might expose cladding to temperatures >100°C. Temperatures might also exceed 100°C in individual rods that are uncovered in the unsaturated alluvium repository post-evaporation.

2.2.14 Mechanical Impact on Cladding

At Yucca Mountain, severe seismic events occurring at a frequency of 1.1×10^{-6}/yr were assumed to fail all the cladding (CRWMS M&O 2000b). Static loading from rockfalls was assumed to fail cladding beginning when open patches made up 50% of the waste package surface, thereby allowing static loading of the rods.

2.2.15 Diffusion-Controlled Cavity Growth in Cladding

Diffusion-controlled cavity growth is the development of microcavities at high temperatures and stresses on grain boundaries causing the separation of the latter. The theory is that metallic materials subjected to high temperatures and stress might develop microcavities on grain boundaries, leading to decohesion of the metal grains. While the concept of diffusion-controlled cavity growth has been hypothesized, the process has never observed in Zr-based cladding (EPRI 2020).

Lastly, nodular corrosion and crud-induced localized corrosion of Zircaloy requires copper (Fraker 1989), a material planned for exclusion from waste packages in the US. Nodular corrosion also requires temperatures greater than 450°C (IAEA 1998), higher than would be achieved in a repository even if a criticality event occurred. Therefore, a postulated criticality event will have no impact on diffusion-controlled cavity growth .

2.2.16 Fluoride-Enhanced Corrosion of Cladding

Fluoride can accelerate Zircaloy corrosion, but to do so the fluoride must be concentrated to higher levels, usually by evaporation (e.g., BSC 2004a). Evaporative concentration of fluoride can occur in the unsaturated alluvium repository where cyclic wetting and drying might occur; however, this repeated evaporative cycle does not occur in a saturated shale repository. CRWMS M&O (2000a) reviewed experimental data on nuclear and non-nuclear corrosion tests of Zircaloy and found that fluoride accelerates general corrosion, especially at low pH; all other halides prompt pitting. General corrosion of Zircaloy is accelerated by hydrofluoric acid, HF, the dissolved form of fluoride below a pH of 3.2 at 25°C. For a pH above 3.2, fluoride is present in solution primarily as fluoride ion, F^-, or alkali fluoride complexes, e.g., CaF^+. The fluoride effect on Zircaloy degradation is pronounced at low pH with most fluoride being present in the acid form, HF.

CRWMS M&O (2000a) determined that if the pH is below 3.2 and the fluoride level is above 5 ppm, the cladding degradation rate can be calculated with the following expression (CRWMS M&O 2000a, Equation 5):

$$\text{Log (corrosion rate in mm/yr)} = 1.51 - 0.661\ \text{pH} + 0.678\ \log[F^-] - 0.599\ \log[Cl^-] \qquad \textit{Equation 13}$$

where the bracketed terms are concentrations in ppm.

At the near-neutral pH of the unsaturated alluvium and saturated shale repositories (Price et al. 2020), the fluoride effect is expected to be sharply diminished because of the low activity of HF. Table 3 lists the near-neutral pH Zircaloy degradation rates in the presence of fluoride cited in CRWMS M&O (2000a). The HF activities in Table 3 were calculated with PHREEQC (Parkhurst and Appelo 1999) assuming equilibrium precipitation of CaF_2 and MgF_2.

Table 3. Low Temperature, Near-Neutral pH Zirconium Degradation Rates in the Presence of Fluoride

pH	Temperature (°C)	Solution (mg/L)	HF activity	Corrosion Rate (μm/yr)
5	55	5,000 NaF	2.4×10^{-6}	8
5	55	1,000 NaF + 4,000 CaF_2	1.9×10^{-6}	6
6.5	55	1,000 NaF	6.1×10^{-8}	6
7	100	100 NaF[a]	1.5×10^{-6}	8

NOTE: All solutions were 1.5% $CaCl_2$ + 1.5% NaCl + 1.0% $MgCl_2$ + 1.0% KCl except for the bottom solution, which was "City Water" (assumed to be distilled water in the subsequent calculations).

[a]Approximately the same rate was measured when fluoride was added as sodium monofluorophosphate.

Source: CRWMS M&O 2000a.

CRWMS M&O (2000a) concluded "If the pH is greater than 3.18 and the fluoride concentration is less than 5 ppm, then Hillner's equation can be used at any temperature." At 55°C–100°C, Hillner's equation (i.e., the general corrosion rate law of Hillner et al. (1998) shown in Equation 3) would predict far lower Zircaloy corrosion rates in the absence of HF (4×10^{-7} to 2×10^{-5} μm/yr) than the corrosion rates in the presence of HF shown in Table 3. The 5- to 7-order-of-magnitude difference in rate between HF-absent dissolution and dissolution in the presence of only micromolar activities of HF suggests one or more of the following possibilities: (1) HF is extremely effective at dissolving Zircaloy, (2) the rates cited in CRWMS M&O (2000a) measured the early, accelerated 'cubic' rates, or (3) another HF-free general corrosion mechanism besides the one measured by Hillner et al. (1998) operates at low temperatures. Note that the Hillner rate law is extensively calibrated but only at high temperatures (>270°C). For comparison, Jerden et al. (2020) used an electrochemical technique—as opposed to weight gain measurements considered by CRWMS M&O (2000a)—to measure a Zircaloy corrosion rate under the following conditions: HF-free, 25°C, pH 7, and [NaCl] = 0.0043M. The measured Zircaloy corrosion rate was 0.19 $g/m^2{\cdot}yr$, which is equivalent to 0.03 μm/yr. Smith (1988) conducted electrochemical scoping experiments and observed effectively no general corrosion (<0.1 μm/yr) at 90°C in tuff-equilibrated J-13 water. Smith (1998) stated that "[t]he results suggest that the very slow oxidative corrosion predicted by extrapolation of higher temperature oxidation models to this lower temperature condition may be of the correct order of magnitude."

Sorting out if, and how, evaporatively concentrated waters might reach pH<3.18 and fluoride levels might exceed 5 ppm is key to predicting accelerated cladding corrosion in the unsaturated alluvium repository (Hardin et al. 2019). PHREEQC calculations of baseline (noncritical) reaction of Al and steels with alluvial groundwaters subject to evaporation at 50°C predict an in-package fluid with a pH range of 7.6<pH<8.4. Fluoride levels reach approximately 100 ppm when the incoming water is evaporated fifty-fold. Corrosion products and secondary phases allowed to form upon equilibration in the calculation were the following: NiO, chromite, hematite, magnetite, boehmite, trevorite, Ni_3S_2, quartz, pyrite, pyrhhotite, chrysotile, calcite, brucite, and the fluoride minerals fluorite and sellaite. The P_{CO2} was set to $10^{-2.5}$ consistent with observed elevated soil and groundwater CO_2 levels. The partial pressure of oxygen was set to 10^{-20} atm to reflect the observed range of redox state of groundwaters, $0<E_H<300$ mV. The specific water composition used in the calculation was that of Ue5ST-1 115.0-115.25, taken from Estrella et al. (1993) and cited as an example of Great Basin alluvial waters by Mariner et al. (2018). Fluoride levels were set to 2.2 ppm, that of J-13 well water at Yucca Mountain. The geochemical calculations indicate that high fluoride concentrations are achievable through evaporative concentration, but low pH is not.

Predicting the likely fluoride levels of in-package fluids requires an explicit understanding of the geochemistry of the geologic setting under consideration. This report focuses on unsaturated alluvium and saturated shale repositories because the potential criticality consequences related to direct DPC disposal have been studied for those geologies. However, salt and crystalline host rocks have been considered in DOE research on other generic repositories (e.g., Mariner et al. 2019). In general, the fluids in geologies other than crystalline host rock are likely to have low, rather than high, fluoride levels because of low availability and/or the formation of fluoride salts, such as fluorite, CaF_2. For example, fluorite-saturated fluoride levels in Opalinus Shale waters are calculated to be ~2.4 ppm; the actual fluoride levels are 0.2–0.6 ppm (Pearson et al. 2003). Brines from the salt host rock at the Waste Isolation Pilot Plant (WIPP) contain 0.9–4.3 ppm fluoride (Popielak et al. 1983). In contrast, crystalline waters typically have elevated fluoride levels, up to 20 ppm, because of the presence of fluoride-bearing biotite and amphiboles (Edmunds and Smedley 2013). Though not typical, fluids in an unsaturated alluvium repository can also develop higher fluoride levels if there is sufficient evaporative concentration due to cyclic wetting and drying (e.g., BSC 2004a).

Even if fluids in an alluvium or crystalline repository have a high fluoride concentration, that fluoride needs to be in the right form (i.e., HF) for fluoride-enhanced corrosion to occur, hence the low pH requirement. In general, in-package pHs in an alluvium repository are expected to be buffered to near neutral by reactions with steel corrosion products (e.g., Price et al. 2020). The same situation exists for crystalline repositories. PHREEQC (Parkhurst and Appelo 1999) calculations were done reacting crystalline waters with waste package steels and allowing corrosion products to form at 50°C. The predicted in-package pHs were 7–9, well above the range at which HF forms. A study conducted by Sandia National Laboratories (SNL 2007b) noted the low potential for acidity production by corroding waste package materials, which is consistent with the PHREEQC outputs.

Hydrolytic production of nitric acid by a postulated criticality event was estimated by Price et al. (2020) to cause no significant change in in-package pH in the unsaturated alluvium repository from near-neutral conditions primarily because of pH buffering by corrosion products inside the package. This result means that the maximal Zircaloy degradation rate in the unsaturated alluvium repository with a postulated criticality event will be approximately those in Table 3 (~7 μm/yr). In the absence of a criticality event, the rates will be effectively zero, i.e., the much lower rate for general corrosion predicted by Equation 3.

Besides the two chemical conditions—high fluoride levels and low pH—required for fluoride-enhanced corrosion, there is a third condition required: a physical pathway allowing the groundwater to have sufficient contact with cladding inside a breached waste package. If these three conditions are met, fluoride-enhanced corrosion could cause significant cladding degradation in an unsaturated alluvium repository under nominal conditions as well as conditions associated with an in-package, steady-state criticality event.

2.3 Summary of Evaluation Results

In Section 2.2, a total of 16 cladding degradation mechanisms were evaluated according to the conditions and limitations described in Section 2.1.1 and Section 2.1.3, respectively. The evaluation results were analyzed to determine which mechanisms should be included in a cladding degradation model that accounts for the physical and chemical environment expected for direct DPC disposal, including conditions arising from an in-package, steady-state criticality event.

Two of the mechanisms—degradation of cladding from waterlogged rods (Section 2.2.1) and degradation of cladding prior to disposal (Section 2.2.2)—occur before disposal and as such would not be affected by conditions after emplacement. According to Section 2.2.2, a small fraction of cladding (<0.1%) will be failed in the reactor or in storage, before it is disposed of in a repository. This early cladding failure should be considered in a cladding degradation model.

The mechanism for mechanical impact on cladding (Section 2.2.14) involves analysis of mechanical damage from seismic events and rockfall. Developing a model suitable for analyzing this type of mechanical damage is outside the scope of this report, so this mechanism is excluded from consideration as a candidate for inclusion in a cladding degradation model.

The remaining 13 cladding degradation mechanisms are listed in Table 4. The mechanisms are binned according to general characterizations of probability and consequence: (1) unlikely (blue), (2) little/no effect or too slow (green), or (3) potentially significant (gold). The binning differentiates between the two geologic reference cases as well as whether nominal conditions or conditions for an in-package, steady-state criticality event apply.

As seen in Table 4, general corrosion and fluoride-enhanced corrosion are deemed potentially significant enough to warrant consideration as candidates for inclusion in a cladding degradation model. In addition, degradation of cladding prior to disposal should be considered for model inclusion. The following is a brief description of the three candidate degradation mechanisms:

- **Early Cladding Failure (i.e., Degradation of Cladding Prior to Disposal, Section 2.2.2)**—The evaluation of this mechanism focuses on cladding failures that occur during reactor operations, pool storage, dry storage, handling/consolidation, and transportation. The early failure of cladding before disposal from all sources is estimated at <0.1%.
- **General Corrosion (Section 2.2.3)**—This mechanism is the primary cladding degradation pathway for fuel in a DPC undergoing a steady-state criticality event in a saturated shale repository. General corrosion is expected to occur due to the criticality-induced high temperatures in a saturated shale repository. Note that the predicted temperatures under nominal conditions for either geologic case or for the unsaturated alluvium repository with a steady-state criticality event are too low for general corrosion to be significant.
- **Fluoride-Enhanced Corrosion (Section 2.2.16)**—This mechanism is expected to be the primary degradation pathway in an unsaturated alluvium repository under nominal conditions as well as conditions associated with an in-package, steady-state criticality event. However, for fluoride-enhanced corrosion to occur, three conditions must be met: (1) fluoride concentration must be elevated (>5 ppm), (2) pH must be low (<3.2), and (3) there must be a physical pathway allowing for sufficient water contact with cladding inside a breached waste package. If all three of these conditions are met, the resulting corrosion could be potentially significant enough to warrant inclusion in a cladding degradation model. Temperatures do not matter in this instance because fluoride-enhanced corrosion can occur in low or high temperatures.

Section 3 describes the conceptual model for these candidate degradation mechanisms as well as initial recommendations for cladding degradation modeling procedures accommodating the mechanisms.

Table 4. Binning of Selected Cladding Degradation Mechanisms

Degradation Mechanism	Unsaturated Alluvium		Saturated Shale	
	Nominal (no criticality event)	Steady-State Criticality Event	Nominal (no criticality event)	Steady-State Criticality Event
General Corrosion	too slow	too slow	too slow	potentially significant
Microbially Influenced Corrosion	unlikely	unlikely	unlikely	unlikely
Localized (Radiolysis Enhanced) Corrosion	unlikely	unlikely	unlikely	unlikely
Localized (Pitting) Corrosion	unlikely	unlikely	unlikely	unlikely
Localized (Crevice) Corrosion	unlikely	unlikely	unlikely	unlikely
Enhanced Corrosion from Dissolved Silica	unlikely	unlikely	unlikely	unlikely
Creep Rupture	little/no effect	little/no effect	little/no effect	little/no effect
Internal Pressurization	little/no effect	little/no effect	little/no effect	little/no effect
Stress Corrosion Cracking	unlikely	unlikely	unlikely	unlikely
Hydride Cracking	unlikely	unlikely	unlikely	unlikely
Cladding Unzipping	too slow	too slow	unlikely	unlikely
Diffusion-Controlled Cavity Growth	unlikely	unlikely	unlikely	Unlikely
Fluoride-Enhanced Corrosion	potentially significant	potentially significant	unlikely	unlikely

NOTE: blue = unlikely (probability)
green = little/no effect or too slow (consequence)
gold = potentially significant (probability and/or consequence)

These designations are based on current understanding of cladding degradation mechanisms. As such, the designations are subject to limitations reflecting the existing areas of uncertainty.

This page is intentionally left blank.

3. CLADDING DEGRADATION MODEL

One of the goals of this research is to advance the development of a cladding degradation model that accounts for the physical and chemical environment expected for direct disposal of DPCs. The relevant conditions include those arising from an in-package, steady-state criticality event. As discussed in Section 2.3, the evaluation of cladding degradation mechanisms identified three mechanisms potentially significant enough to consider as candidates for incorporation into a cladding degradation model. Section 3.1 briefly describes the conceptual model for the candidate mechanisms, and Section 3.2 presents the recommendations for cladding degradation modeling procedures addressing the mechanisms.

3.1 Conceptual Model for Candidate Cladding Degradation Mechanisms

Early cladding failure, general corrosion, and fluoride-enhanced corrosion were identified as candidate mechanisms for inclusion in a cladding degradation model (Section 2.3). The discussion of the conceptual model below provides a description of the candidate cladding degradation mechanisms, the potential events after cladding failure, and a brief summary of the conceptual model. Further details about the mechanisms are located in the sections for the individual evaluations (Section 2.2.2 for early cladding failure, Section 2.2.3 for general corrosion, and Section 2.2.16 for fluoride-enhanced corrosion).

Early Cladding Failure—A small amount of cladding (<0.1%) is expected to fail before disposal. The estimate includes cladding failures that occur during reactor operations, pool storage, dry storage, handling/consolidation, and transportation.

General Corrosion—If cladding failure occurs, general corrosion is expected to be the primary driver rather than other mechanisms such as SCC, DHC, creep failure, pitting and crevice corrosion, or rod pressurization because the latter are very unlikely to occur or the potential effects are too small (Table 4). However, the cladding degradation rate due to general corrosion is expected to be significant only in high temperature regimes. If DPCs are disposed directly in a repository and a breached DPC experiences a steady-state criticality event, this criticality event would result in increased temperatures even after the thermal period.

As discussed in Section 2.1.1, the criticality consequences associated with direct DPC disposal have been studied for a saturated shale repository and an unsaturated alluvium repository. Price et al. (2020) determined that an in-package, steady-state criticality event lasting 10,000 years in a saturated geologic repository could cause temperatures to reach about 250°C for a prolonged period of time; the expected peak temperatures in an unsaturated alluvium repository are not expected to exceed 100°C. As a result, general corrosion is significant when a prolonged, in-package, steady state criticality event occurs in a saturated shale repository, but not in an unsaturated alluvium repository. Further research would be needed to determine is general corrosion is significant for the disposal concepts in geologies other than saturated shale and unsaturated alluvium.

Zircaloy degradation rates from general corrosion can be calculated using Equation 3, which was developed by Hillner et al. (1998). However, an irradiation multiplier of at least 2 is often used to account for the fact that irradiated Zircaloy degrades faster than nonirradiated Zircaloy. Using a multiplier of 2 results in a degradation rate on the order of 0.34 μm/yr for general corrosion at 250°C (approximate peak temperature for an in-package, steady-state criticality event in a saturated shale repository). Table 5 gives the associated time required for Zircaloy in cladding, grid spacer walls, and guide tubes in a 17×17 PWR fuel rod array to dissolve completely by general corrosion at 250°C (Price et al. 2020, Table 7-1).

Table 5. Zircaloy Thicknesses and Failure Times at 250°C

Component	Thickness (mils)	Failure Time (years)
Cladding	22.5[a]	1,640[b]
Grid Spacer Walls	10[c]	366[d]
Guide Tubes	16[c]	585[d]

NOTE/Source: [a]Westinghouse Electric Company LLC 2011
[b]Outside-in corrosion only.
[c]Fascitelli and Durbin 2020, personal communication.
[d]Corrosion from both sides.

The results in Table 5 indicate that, a few hundred years after onset of an in-package, steady-state criticality event in a saturated shale repository, complete general corrosion of fuel assembly grid spacer walls and guide tubes will result in settling of fuel rods upon each other. This rod consolidation could exclude the water moderator and might terminate a postulated criticality event (Alsaed 2020), though it will depend upon the final configuration of the rods. Note that the Zircaloy failure times calculated above are maxima for overall failure; since "gross damage will ensue when the surface retreat reaches approximately half the thickness" (Hardin et al. 2019).

Fluoride-Enhanced Corrosion—Although general corrosion of Zircaloy is usually negligible at low temperatures, fluoride in high enough concentrations (>5 ppm) can accelerate general corrosion even at low temperatures (CRWMS M&O 2000). Hydrofluoric acid, HF—the dissolved form of fluoride that drives fluoride-enhanced corrosion—occurs below a pH of 3.2 at 25°C. For a pH above 3.2, fluoride is present in solution primarily as fluoride ion, F^-, or alkali fluoride complexes, e.g., CaF^+. Three conditions must be met for fluoride-enhanced corrosion to occur: (1) fluoride concentration must be elevated (>5 ppm), (2) pH must be low (<3.2), and (3) there must be a physical pathway for sufficient water contact with cladding inside a breached waste package.

If the three conditions are met in an unsaturated alluvium repository, fluoride-enhanced corrosion is expected to be the primary degradation pathway for cladding under nominal conditions or if a criticality event occurs. If an in-package, steady-state criticality event does occur in an unsaturated alluvium repository, the slightly higher (<100°C) temperatures (Price et al. 2020) would accelerate fluoride-enhanced corrosion. This degradation mechanism is not expected to be a significant factor in a saturated shale repository, with or without a criticality event.

Events after Cladding Failure—Once cladding is completely degraded all fuel is generally assumed to be exposed to the in-package environment in performance assessment calculations (BSC 2004b). Any fission gas in the gap between the cladding and the fuel is assumed to be released. If water is present below its boiling point, spent fuel is assumed to be completely exposed to corrosion. Two pathways for fuel exposure might occur by including unzipping in oxidizing environments and/or fuel side corrosion of cladding. Formation of high-volume fuel corrosion products under oxidizing conditions unpeels initially failed cladding during unzipping. Fuel side corrosion of cladding involves formation of high volume ZrO_2, which might similarly split degraded cladding.

Alternatively, corrosion products might "self-seal" the underlying rods and stop radionuclide release from rods by preventing further access of water and oxygen.

Summary—Cladding failure is the first step to spent fuel degradation and radionuclide release from a repository. A small fraction of cladding (<0.1%) is expected to fail during reactor operations, pool storage, dry storage, handling/consolidation, and transportation, before disposal in a repository. Upon disposal, general corrosion can fail cladding if repository temperatures are elevated for long periods of time. Below about 100°C, general corrosion can fail cladding during the regulatory period if there is fluoride-enhanced corrosion, which occurs only if the cladding is exposed to waters containing evaporatively concentrated dissolved fluoride >5 ppm and having a pH below 3.2. If cladding is failed, spent fuel can be conservatively assumed to be fully exposed to the in-package environment (e.g., BSC 2004b), allowing degradation of the fuel as well as release of fission product gases.

3.2 Recommendations for Cladding Degradation Modeling Procedures

Given the conceptual model outlined in Section 3.1, a cladding degradation model needs to have the capability to do the following: (1) account for early failure of cladding, (2) calculate baseline cladding degradation rates due to general corrosion, (3) predict in-package fluoride levels and pH to check if chemical conditions for fluoride-enhanced corrosion are met, and (4) if warranted by fluoride levels and pH, calculate degradation rates due to fluoride-enhanced corrosion.

As described in the conceptual model, accurate estimation of low temperature cladding degradation due to fluoride-enhanced corrosion also requires a physical pathway for sufficient contact of high fluoride, low pH water with cladding inside a breached waste package. Additional research involving actual observations of physical flow and accelerated degradation would help refine the modeling approach.

Based on the current level of knowledge, the procedures below are recommended for the mathematical aspects of modeling cladding degradation to support a performance assessment. Note that the procedures are independent of the geologic setting or whether a criticality event has or has not occurred. These factors affect the values of the inputs, but not the procedures themselves.

Step 1—Assume 0.1% of cladding will be degraded predisposal and will fully unzip in the repository.

Step 2—Use Equation 3 (the rate law of Hillner et al. [1998]) to calculate the baseline cladding degradation rate due to general corrosion at all temperatures:

$$\Delta W = 3.47 \times 10^{7} \exp\left[\frac{-11{,}452}{T}\right] \times t \qquad \textit{Equation 3 (repeated)}$$

where ΔW = ZrO_2 weight gain (mg/dm^2), T = absolute temperature (K), and t = exposure time (days).

Step 3—Check the likelihood of fluoride-enhanced corrosion using a parallel reaction-path calculation to predict pH and fluoride levels that result when repository horizon fluids are equilibrated with waste package steels and their corrosion products; the calculation is described in Section 2.2.16.

Step 4—If calculated pH is above 3.2 and/or fluoride is below 5 ppm, then the conditions for fluoride-enhanced corrosion are not met, and the baseline cladding degradation rate calculated with Equation 3 in Step 2 is used. However, if calculated pH is below 3.2 and fluoride is above 5 ppm, then the conditions for fluoride-enhanced corrosion are met, and the cladding degradation rate is calculated with the following expression (CRWMS M&O 2000, Equation 5):

$$\text{Log (corrosion rate in mm/yr)} = 1.51 - 0.661\ \text{pH} + 0.678\ \log[F^-] - 0.599\ \log[Cl^-] \qquad \textit{Equation 13 (repeated)}$$

The bracketed terms are concentrations in ppm.

This page is intentionally left blank.

4. REFERENCES

Alsaed, A. 2020. *Permanent Criticality Termination Processes in Disposed DPCs.* M4SF-20SN010305063; SAND2020-6615 R. Albuquerque, NM: Sandia National Laboratories.

Alsaed, A. and L.L. Price. 2020. *Features, Events, and Processes Relevant to DPC Disposal Criticality Analysis.* SAND2020-9165. Albuquerque, NM: Sandia National Laboratories.

Billone, M.C. and T.A. Burtseva. 2020. *Preliminary Destructive Examination Results for Sibling Pin Cladding.* M2SF-20AN010201019; ANL-19/53 Rev 2. Argonne, IL: Argonne National Laboratory.

Brady, P.V., B.W. Arnold, G.A. Freeze, P.N. Swift, S.J. Bauer, J.L. Kanney, R.P. Rechard, and J.S. Stein. 2009. *Deep borehole disposal of high-level radioactive waste*. SAND2009-4401. Albuquerque, NM: Sandia National Laboratories.

BSC (Bechtel SAIC Company). 2004a. *Clad Degradation – FEPs Screening Arguments*. ANL-WIS-MD-000008 REV01. Las Vegas, NV: Bechtel SAIC Company.

BSC. 2004b. *CSNF Waste Form Degradation: Summary Abstraction*. ANL-EBS-MD-000015 REV 02. Las Vegas, NV: Bechtel SAIC Company.

Carbol, P., J. Cobos-Sabate, J.-P. Glatz, C. Ronchi, V. Rondinella, D.H. Wegen, T. Wiss, A. Loida, V. Metz, B. Kienzler, K. Spahiu, B. Grambow, J. Quiñones, and A0. Martinez Esparza Valiente. 2005. *The effect of dissolved hydrogen on the dissolution of 233U doped UO2(s) high burn-up spent fuel and MOX fuel*, ed. K. Spahiu. SKB TR-05-09. Stockholm, Sweden: Svensk Kärnbränslehantering AB (Swedish Nuclear Fuel and Waste Management Co).

CRWMS (Civilian Radioactive Waste Management System) M&O (Management and Operating Contractor). 2000a. *Clad Degradation - Local Corrosion of Zirconium and Its Alloys under Repository Conditions*. ANL-EBS-MD-000012 REV 00. Las Vegas, NV: US Department of Energy, Office of Civilian Radioactive Waste Management System Management and Operating Contractor.

CRWMS M&O. 2000b. *Clad Degradation – Summary and Abstraction*. ANL-WIS-MD-000007 REV00. Las Vegas, NV: US Department of Energy, Office of Civilian Radioactive Waste Management System Management and Operating Contractor.

CRWMS M&O. 2000c. *Creep Strain Values and Correlation for Irradiated Spent Nuclear Fuel*. Input Transmittal PA-WP-00383.Ta. Las Vegas, NV: US Department of Energy, Office of Civilian Radioactive Waste Management System Management and Operating Contractor.

CRWMS M&O. 2000d. *Initial Cladding Condition*. ANL-EBS-MD-000048 REV00 ICN01. Las Vegas, NV: US Department of Energy, Office of Civilian Radioactive Waste Management System Management and Operating Contractor.

CRWMS M&O. 2001. *Creep Strain Correlation for Irradiated Cladding*. CAL-EBS-MD-000015 REV 00. Las Vegas, NV: US Department of Energy, Office of Civilian Radioactive Waste Management System Management and Operating Contractor.

DOE (US Department of Energy). 2008. *Yucca Mountain Repository License Application*. DOE/RW-0573, Rev. 1. Las Vegas, NV: US Department of Energy, Office of Civilian Radioactive Waste Management.

Edmunds, W.M. and P.L. Smedley. 2013. Fluoride in natural waters. In *Essentials of Medical Geology*, ed. O. Selinus, 311–336. New York, NY: Springer. https://doi.org/10.1007/978-94-007-4375-5_13.

Einziger, R.E. and R.V. Strain. 1986. Behavior of Breached Pressurized Water Reactor Spent-Fuel Rods in an Air Atmosphere between 250 and 360°C. *Nuclear Technology* 75 (1): 82–95. https://doi.org/10.13182/NT86-A15979.

EPRI (Electric Power Research Institute). 2008. Executive Summary to *The Path to Zero Defects: EPRI Fuel Reliability Guidelines*. Palo Alto, CA: Electric Power Research Institute. http://mydocs.epri.com/docs/CorporateDocuments/SectorPages/Portfolio/PDM/FRP%20Exec%20Sum1c.pdf.

EPRI. 2013. *End-of-Life Rod Internal Pressures in Spent Pressurized Water Reactor Fuel.* 3002001949. Palo Alto, CA: Electric Power Research Institute.

EPRI. 2020. *Phenomena Identification and Ranking Table (PIRT) Exercise for Used Fuel Cladding Performance*. 3002018439. Palo Alto, CA: Electric Power Research Institute.

Estrella, R., S. Tyler, J. Chapman, and M. Miller. 1993. *Area 5 Site Characterization Project: Report of hydraulic property analysis through August 1993*. DOE/NV/10845-41. Las Vegas, NV: University of Nevada, Desert Research Institute.

Fahey, J., D. Holmes, and T.-L. Yau. 1997. Evaluation of localized corrosion of zirconium in acidic chloride solutions. *Corrosion* 53 (1): 54–61.

Fascitelli, D. and S. Durbin. 2020. Fuel assembly dimensions. Personal communication.

Fraker, A. 1989. *Corrosion of Zircaloy Spent Fuel Cladding in a Repository*. NISTIR 89-4114. Gaithersburg, MD: US Department of Commerce, National Institute of Standards and Technology.

Hardin, E., B. Damjanac, J. Furtney, A. Riahi, and Varun. 2019. *DPC Criticality Simulation Preliminary Phase: Fuel/Basket Degradation Models*, ed. E. Hardin. M3SF-19SN010305071. Albuquerque, NM: Sandia National Laboratories.

Hardin, E. and E. Kalinina. 2016. *Cost Estimation Inputs for Spent Nuclear Fuel Geologic Disposal Concepts*. SAND2016-0235. Albuquerque, NM: Sandia National Laboratories.

Hardin, E., L. Price, E. Kalinina, T. Hadgu, A. Ilgen, C. Bryan, J. Scaglione, K. Banerjee, J. Clarity, R. Jubin, V. Sobes, R. Howard, J. Carter, T. Severynse, and F. Perry. 2015. *Summary of Investigations on Technical Feasibility of Direct Disposal of Dual-Purpose Canisters*. FCRD-UFD-2015-000129, Rev. 0; SAND2015-8712R. Albuquerque, NM: Sandia National Laboratories. doi: 10.2172/1504860.

Harrar, J.E., J. Carley, W.F. Isherwood, and E. Raber. 1990. *Report of the Committee to Review the Use of J-13 Well Water in Nevada Nuclear Waste Storage Investigations*. UCID-21867. Livermore, CA: Lawrence Livermore National Laboratory. https://doi.org/10.2172/137644.

Henningson, P., J. Willse, B. Cox, M. Bale, K. Murty, and W. Pavinich. 1998. *Cladding Integrity Under Long Term Disposal*. 51-1267509-00. Lynchburg, VA: Framatome Technologies.

Hillner, E. 1977. Corrosion of zirconium-base alloys: an overview. STP35573S. In *Zirconium in the Nuclear Industry*, ed. P. Lowe, Jr., 211–235. West Conshohocken, PA: American Society of Test Materials (ASTM). https://doi.org/10.1520/STP35573S.

Hillner, E., D. Franklin, and J. Smee. 1998. *The Corrosion of Zircaloy-Clad Fuel Assemblies in a Geologic Repository Environment*. WAPD-T-3173. West Mifflin, PA: Bettis Atomic Power Laboratory.

IAEA (International Atomic Energy Agency). 1988. *Survey of Experience with Dry Storage of Spent Nuclear Fuel and Update of Wet Storage Experience*. Technical Report Series No. 290. Vienna, Austria: International Atomic Energy Agency.

IAEA. 1998. *Waterside corrosion of zirconium alloys in nuclear power plants*. IAEA-TECDOC-996. Vienna, Austria: International Atomic Energy.

Jerden, J., K. Frey, and W. Ebert. 2015. A multiphase interfacial model for the dissolution of spent nuclear fuel. *Journal of Nuclear Materials* 462 (July): 135–146. https://doi.org/10.1016/j.jnucmat.2015.03.036.

Jerden, J., S. Thomas, E. Lee, V.K. Gattu, and W. Ebert. 2020. *Results from Fuel Matrix Degradation Model Parameterization Experiments and Model Development Activities*. ANL/CFCT-20/15. Argonne, IL: Argonne National Laboratory.

Johnson, A.B. 1977. *Behavior of Spent Nuclear Fuel in Water Pool Storage*. BNWL-2256. Richland, WA: Pacific Northwest Laboratory. https://doi.org/10.2172/7284014.

Johnson, A. and E. Gilbert. 1983. *Technical basis for storage of Zircaloy-clad spent fuel in inert gases*. Richland, WA: Pacific Northwest Laboratory. https://doi.org/10.2172/713558.

Kalinina, E., D. Ammerman, C. Grey, M. Arviso, C. Wright, L. Lujan, S. Saltzstein, S. Ross, N. Klymshyn, B. Hanson, A. Alonso, I. Perez, R. Garmendia, G. Calatuyad, and W. Choi. 2019. International Multi-Modal Spent Nuclear Fuel Test Transportation Test: The Transportation Test Triathlon. Paper presented at the International Conference on the Management of Spent Fuel from Nuclear Power Reactors held June 24–28, 2019 in Vienna, Austria. SAND2019-1995C; IAEA-CN-123/45. Albuquerque, NM: Sandia National Laboratories.

Mardon, J.P., G.L. Garner, and P.B. Hoffmann. 2010. M5® a Breakthrough in Zr Alloy. In *LWR Fuel Performance/TopFuel/WRFPM 2010: Orlando, Florida, USA, 26–29 September 2010*, 577–586. LaGrange Park, IL: American Nuclear Society.

Mariner, P.E., E.R. Stein, J.M. Frederick, S.D. Sevougian, and G.E. Hammond. 2017. *Advances in Geologic Disposal System Modeling and Shale Reference Case*. SFWD-SFWST-2017-000044; SAND2017-10304R. Albuquerque, NM: Sandia National Laboratories.

Mariner, P.E., E.R. Stein, S.D. Sevougian, L.J. Cunningham, J.M Frederick, G.E. Hammond, T.S. Lowry, S. Jordan, and E. Basurto. 2018. *Advances in Geologic Disposal Safety Assessment and an Unsaturated Alluvium Reference Case*. SFWD-SFWST-2018-000509; SAND2018-11858R. Albuquerque, NM: Sandia National Laboratories.

Mariner, P.E., L.A. Connolly, L.J. Cunningham, B.J. Debusschere, D.C. Dobson, J.M. Frederick, G.E. Hammond, S.H. Jordan, T.C. LaForce, M.A. Nole, H.D. Park, F.V. Perry, R.D. Rogers, D.T. Seidl, S.D. Sevougian, E.R. Stein, P.N. Swift, L.P. Swiler, J. Vo, and M.G. Wallace. 2019. *Progress in Deep Geologic Disposal Safety Assessment in the U.S. since 2010.* SAND2019-12001 R; M2SF-19SN010304041. Albuquerque, NM: Sandia National Laboratories.

McNeil, M.B. and A. Odom. 1994. Thermodynamic Prediction of Microbiologically Influenced Corrosion (MIC) by Sulfate-Reducing Bacteria (SRB). In *Microbiologically Influenced Corrosion Testing*, 173–179. Materials Park, OH: ASTM International. doi: 10.1520/STP12933S.

NRC (US Nuclear Regulatory Commission). 2019. *Managing Aging Processes in Storage (MAPS) Report*. NUREG-2214. Washington, D.C.: US Nuclear Regulatory Commission, Office of Nuclear Material Safety and Safeguards.

Pan, G., A.M. Garde, A.R. Atwood, R. Källström, and D. Jädernäs. 2013. High Burnup Optimized ZIRLO Cladding Performance. Paper 8427 in *LWR Fuel Performance Meeting (Top Fuel 2013): Charlotte, North Carolina, USA, 15–19 September*, 1–8. LaGrange Park, IL: American Nuclear Society.

Parkhurst, D.L. and C.A.J. Appelo. 1999. *User's Guide to PHREEQC (Version 2) – A Computer Program for Speciation, Batch-Reaction, One-Dimensional Transport, and Inverse Geochemical Calculations*. Water-Resources Investigations Report 99-4259. Reston, VA: US Geological Survey.

Pearson, F.J., D. Arcos, A. Bath, J.Y. Boisson, A.M. Fernández, H.-E. Gäbler, E. Gaucher, A. Gautschi, L. Griffault, P. Hernán, and H.N. Waber. 2003. *Geochemistry of Water in the Opalinus Clay Formation at the Mont Terri Rock Laboratory*. Report of the Federal Office for Water and Geology (FOWG), Geology Series No. 5. Bern, Switzerland: Federal Office for Water and Geology.

Pescatore, C., M.G. Cowgill, and T.M. Sullivan. 1990. *Zircaloy cladding performance under spent fuel disposal conditions*. BNL-52235. Upton, NY: Brookhaven National Laboratory.

Popielak, R.S., R.L. Beauheim, S.R. Black, W.E. Coons, C.T. Ellingson, and R.L. Olsen. 1983. *Brine reservoirs in the Castile Formation, Waste Isolation Plant Plant (WIPP) project, southeastern New Mexico*. WTSD-TME-3153. Albuquerque, NM: D'Appolonia Consulting Engineers.

Price, L.L., A.A. Alsaed, A. Barela, P.V. Brady, F. Gelbard, M.B. Gross, M. Nole, J.L. Prouty, K. Banerjee, S. Bhatt, G.G. Davidson, Z. Fang, R. Howard, S.R. Johnson, S.L. Painter, M. Swinney, and E. Gonzalez. 2019. *Preliminary Analysis of Postclosure DPC Criticality Consequences*. M2SF-20SN010305061; SAND2020-4106. Albuquerque, NM: Sandia National Laboratories.

Price, L.L., A.A. Alsaed, P.V. Brady, F. Gelbard, V. Mousseau, M. Nole, J.L. Prouty, A. Salazar, K. Banerjee, S. Bhatt, G.G. Davidson, S.L. Painter, M. Swinney, and E. Gonzalez. 2020. *Status Report—Progress in Developing a Repository-Scale Performance Assessment Model*. M4SF-20SN010305064. Albuquerque, NM: Sandia National Laboratories.

Price, L.L., A. Salazar, E. Basurto, A.A. Alsaed, J. Cardoni, M. Nole, J. Prouty, C. Sanders, G. Davidson, M. Swinney, S. Bhatt, E. Gonzalez, and B. Kiedrowski. 2021. *Repository-Scale Performance Anssessment Incorporating Postclosure Criticality.* M2SF-21SN010305061. Albuquerque, NM: Sandia National Laboratories.

S. Cohen & Associates. 1999. *Effectiveness of Fuel Rod Cladding as an Engineered Barrier in the Yucca Mountain Repository*. McLean, VA: S. Cohen & Associates.

Sevougian, S.D., P.E. Mariner, L.A. Connolly, R.J. MacKinnon, R.D. Rogers, D.C. Dobson, J.L. Prouty. 2019. *DOE SFWST Campaign R&D Roadmap Update.* M2SF-19SN010304042, Rev. 1; SAND2019-9033 R. Albuquerque, NM: Sandia National Laboratories.

Shoesmith, D.W. 2013. The chemistry/electrochemistry of spent nuclear fuel as a wasteform. In *Uranium – Cradle to Grave*, eds. P.C. Burns and G.E. Sigmon, 337–368. Mineralogical Association of Canada, Short Course Series 43. Winnipeg, Manitoba: Mineralogical Association of Canada.

SKB (Svensk Kärnbränslehantering AB). 2011. *Long-term safety for the final repository for spent nuclear fuel at Forsmark: Main report of the SR-Site project*, Volume III. Stockholm, Sweden: Svensk Kärnbränslehantering AB (Swedish Nuclear Fuel and Waste Management Co).

Smith, H. 1988. *Electrochemical Corrosion-Scoping Experiments—An Evaluation of the Results*. WHC-EP-0065. Richland, WA: Westinghouse Hanford Co.

SNL (Sandia National Laboratories). 2007a. *Cladding Degradation Summary for LA*. ANL-WIS-MD-000021 REV 03 ADD 01. Las Vegas, NV: Sandia National Laboratories.

SNL. 2007b. *In-Package Chemistry Abstraction*. ANL-EBS-MD-000037 REV 04 ADD 01. Las Vegas, NV: Sandia National Laboratories.

Tasooji, A., R. Einziger, and A. Miller. 1984. Modeling of Zircaloy Stress-Corrosion Cracking: Texture Effects and Dry Storage Spent Fuel Behavior. In *Zirconium in the Nuclear Industry: Sixth International Symposium*, eds. D.G. Franklin and R.B. Adamson, 595–626. Philadelphia, PA: American Society for Testing and Materials (ASTM) International.

Westinghouse Electric Company LLC. 2011. Reactor Vessel and Internals. Section 3.1 of *Westinghouse Technology Systems Manual*. Chattanooga, TN: US Nuclear Regulatory Commission, Human Resources Training & Development.

Yau, T.L. and R.T. Webster. 1987. Corrosion of Zirconium and Hafnium. In *Corrosion*, Volume 13 of *American Society for Metals Handbook,* 9th ed., 707–721. ASM STP 824. Materials Park, OH: American Society for Metals (ASM) International.